serum-free Hank's solution (containing in mM: 125 NaCl, 5.6 glucose, 4.8 KCl, 1. 2 $MgSO_4 \cdot 7H_2O$, 1.2 KH_2PO_4, 1.3 $CaCl_2 \cdot 2H_2O$, 25 *N*-2-hydroxyethylpiperazine-*N'*-2-ethanesulfonic acid (pH 6.0)) for 10 min. The uptake study was started by adding 500 μl of solution containing 30 μM [^{14}C]Gly-Sar to the plate. After 2 min, the cells were washed twice in an ice-cold solution, and lysed in 0.1 N NaOH for 20 min for scintillation counting.

To determine the kinetic parameters, the concentrations of Gly-Sar were varied from 30 to 1000 μM. PEPT2-mediated Gly-Sar uptake was calculated as the difference between the uptake rates into HEK293 cells transiently expressing PEPT2 and those into HEK293 cells transfected with the vector (pcDNA3.1, Invitrogen) only.

Cell surface biotinylation

Surface biotinylation of PEPT2 at the plasma membrane was performed as described elsewhere.[49] Surface proteins in HEK293 cells transfected with pcDNA3.1(+)-hPEPT2 and pcDNA3.1(+)-hPDZK1 or pcDNA3.1(+) empty vector (mock) were biotinylated with Sulfo-NHS-SS-Biotin (Pierce) (0.5 mg/ml) in phosphate-buffered saline for 30 min at 4°C. Cell lysates were then incubated with Ultralink-immobilized NeutrAvidin beads (Pierce) to precipitate biotinylated proteins. PEPT2 was detected with polyclonal PEPT2 antibody (1:10,000).[41]

Statistical analysis

Uptake experiments were conducted three times, and each uptake experiment was performed in triplicate. Values are presented as the mean$\pm$s.e. Statistical significance was determined by Student's *t*-test.

ACKNOWLEDGMENTS

We thank Akie Toki and Keiko Sakama for technical assistance. The anti-hPDZK1 polyclonal antibody was supplied by Transgenic Inc., Kumamoto, Japan. This work was supported in part by grants from the Ministry of Education, Culture, Sports, Science and Technology of Japan, the Japan Society for the Promotion of Science, Research on Health Sciences focusing on Drug Innovation from the Japan Health Sciences Foundation, Mutual Aid Corporation for Private Schools of Japan, the Nakatomi Foundation, the Salt Science Research Foundation (No. 0524), the Japan Foundation of Applied Enzymology, Astellas Foundation for Research on Metabolic Disorders, Gout Research Foundation of Japan, Heiwa Nakajima Foundation, and Health and Labor Sciences Research Grants for Research on Advanced Medical Technology: Toxicogenomics Project. This work was presented in part at the Annual Meeting of Experimental Biology 2004, Washington DC, April 2004, and published in abstract form (*FASEB J* **18**:A695, 2004).

REFERENCES

1. Daniel H, Rubio-Aliaga I. An update on renal peptide transporters. *Am J Physiol Renal Physiol* 2003; **284**: F885–F892.
2. Nielsen CU, Brodin B. Di/tri-peptide transporters as drug delivery targets: regulation of transport under physiological and patho-physiological conditions. *Curr Drug Targets* 2003; **4**: 373–388.
3. Terada T, Inui K. Peptide transporters: structure, function, regulation and application for drug delivery. *Curr Drug Metab* 2004; **5**: 85–94.
4. Boll M, Markovich D, Weber WM *et al.* Expression cloning of a cDNA from rabbit small intestine related to proton-coupled transport of peptides, lactam antibiotics and ACE-inhibitors. *Pflugers Arch* 1994; **429**: 146–149.
5. Fei YJ, Kanai Y, Nussberger S *et al.* Expression cloning of a mammalian proton-coupled oligopeptide transporter. *Nature* 1994; **368**: 563–566.
6. Boll M, Herget M, Wagener M *et al.* Expression cloning and functional characterization of the kidney cortex high-affinity proton-coupled peptide transporter. *Proc Natl Acad Sci USA* 1996; **93**: 284–289.
7. Saito H, Okuda M, Terada T *et al.* Cloning and characterization of a rat H+/peptide cotransporter mediating absorption of β-lactam antibiotics in the intestine and kidney. *J Pharmacol Exp Ther* 1995; **275**: 1631–1637.
8. Miyamoto KI, Shiraga T, Morita K *et al.* Sequence, tissue distribution and developmental changes in rat intestinal oligopeptide transporter. *Biochim Biophys Acta* 1996; **1305**: 34–38.
9. Saito H, Terada T, Okuda M *et al.* Molecular cloning and tissue distribution of rat peptide transporter PEPT2. *Biochim Biophys Acta* 1996; **1280**: 173–177.
10. Liang R, Fei YJ, Prasad PD *et al.* Human intestinal H^+/peptide cotransporter. Cloning, functional expression, and chromosomal localization. *J Biol Chem* 1995; **270**: 6456–6463.
11. Liu W, Liang R, Ramamoorthy S *et al.* Molecular cloning of PEPT2, a new member of the H^+/peptide cotransporter family, from human kidney. *Biochim Biophys Acta* 1995; **1235**: 461–466.
12. Ramamoorthy S, Liu W, Ma YY *et al.* Proton/peptide cotransporter (PEPT2) from human kidney: functional characterization and chromosomal localization. *Biochim Biophys Acta* 1995; **1240**: 1–4.
13. Smith DE, Pavlova A, Berger UV *et al.* Tubular localization and tissue distribution of peptide transporters in rat kidney. *Pharm Res* 1998; **15**: 1244–1249.
14. Ogihara H, Saito H, Shin BC *et al.* Immuno-localization of H^+/peptide cotransporter in rat digestive tract. *Biochem Biophys Res Commun* 1996; **220**: 848–852.
15. Shen H, Smith DE, Yang T *et al.* Localization of PEPT1 and PEPT2 proton-coupled oligopeptide transporter mRNA and protein in rat kidney. *Am J Physiol* 1999; **276**: F658–F665.
16. Rubio-Aliaga I, Frey I, Boll M *et al.* Targeted disruption of the peptide transporter Pept2 gene in mice defines its physiological role in the kidney. *Mol Cell Biol* 2003; **23**: 3247–3252.
17. Takahashi K, Masuda S, Nakamura N *et al.* Upregulation of H(+)-peptide cotransporter PEPT2 in rat remnant kidney. *Am J Physiol Renal Physiol* 2001; **281**: F1109–F1116.
18. Nakamura N, Masuda S, Takahashi K *et al.* Decreased expression of glucose and peptide transporters in rat remnant kidney. *Drug Metab Pharmacokinet* 2004; **19**: 41–47.
19. Wenzel U, Diehl D, Herget M *et al.* Regulation of the high-affinity H+/peptide cotransporter in renal LLC-PK1 cells. *J Cell Physiol* 1999; **178**: 341–348.
20. Bravo SA, Nielsen CU, Amstrup J *et al.* Epidermal growth factor decreases PEPT2 transport capacity and expression in the rat kidney proximal tubule cell line SKPT0193 cl.2. *Am J Physiol Renal Physiol* 2004; **286**: F385–F393.
21. Biber J. Emerging roles of transporter-PDZ complexes in renal proximal tubular reabsorption. *Pflugers Arch* 2001; **443**: 3–5.
22. Levi M. Role of PDZ domain-containing proteins and ERM proteins in regulation of renal function and dysfunction. *J Am Soc Nephrol* 2003; **14**: 1949–1951.
23. Moe OW. Scaffolds: orchestrating proteins to achieve concerted function. *Kidney Int* 2003; **64**: 1916–1917.
24. Anzai N, Jutabha P, Kanai Y, Endou H. Integrated physiology of proximal tubular organic anion transport. *Curr Opin Nephrol Hypertens* 2005; **14**: 472–479.
25. Fanning AS, Anderson JM. Protein modules as organizers of membrane structure. *Curr Opin Cell Biol* 1999; **11**: 432–439.
26. Garner CC, Nash J, Huganir RL. PDZ domains in synapse assembly and signalling. *Trends Cell Biol* 2000; **10**: 274–280.
27. Hung AY, Sheng M. PDZ domains: structural modules for protein complex assembly. *J Biol Chem* 2002; **277**: 5699–5702.
28. Russel FGM, Masereeuw R, van Aubel RAMH. Molecular aspects of renal anionic drug transport. *Annu Rev Physiol* 2002; **64**: 563–594.
29. Anzai N, Miyazaki H, Noshiro R *et al.* The multivalent PDZ domain-containing protein PDZK1 regulates transport activity of renal urate-anion exchanger URAT1 via its C-terminal. *J Biol Chem* 2004; **279**: 45942–45950.
30. Anzai N, Enomoto A, Endou H. Renal urate handling: clinical relevance of recent advances. *Curr Rheumatol Rep* 2005; **7**: 227–234.
31. Kato Y, Yoshida K, Watanabe C *et al.* Screening of the interaction between xenobiotic transporters and PDZ proteins. *Pharm Res* 2004; **21**: 1886–1894.
32. Kocher O, Comella N, Tognazzi K, Brown LF. Identification and partial characterization of PDZK1: a novel protein containing PDZ interaction domains. *Lab Invest* 1998; **78**: 117–125.
33. Hernando N, Wagner CA, Gisler SM *et al.* PDZ proteins and proximal ion transport. *Curr Opin Nephrol Hypertens* 2004; **13**: 569–574.

34. Weinman EJ, Steplock D, Wang Y, Shenolikar S. Characterization of a protein cofactor that mediates protein kinase A regulation of the renal brush border membrane Na^+-H^+ exchanger. *J Clin Invest* 1995; **95**: 2143–2149.
35. Reczek D, Berryman M, Bretscher J. Identification of EBP50: a PDZ-containing phosphoprotein that associates with members of the ezrin-radixin-moesin family. *J Cell Biol* 1997; **139**: 169–179.
36. Hall RA, Ostedgaard LS, Premont RT *et al.* A C-terminal motif found in the beta2-adrenergic receptor, P2Y1 receptor and cystic fibrosis transmembrane conductance regulator determines binding to the Na^+/H^+ exchanger regulatory factor family of PDZ proteins. *Proc Natl Acad Sci USA* 1998; **95**: 8496–8501.
37. Scott RO, Thelin WR, Milgram SL. A novel PDZ protein regulates the activity of guanylyl cyclase C, the heat-stable enterotoxin receptor. *J Biol Chem* 2002; **277**: 22934–22941.
38. Songyang Z, Fanning AS, Fu C *et al.* Recognition of unique carboxyl-terminal motifs by distinct PDZ domains. *Science* 1997; **275**: 73–77.
39. Harris BZ, Lim WA. Mechanism and role of PDZ domains in signaling complex assembly. *J Cell Sci* 2001; **114**: 3219–3231.
40. Kocher O, Comella N, Gilchrist A *et al.* PDZK1, a novel PDZ domain-containing protein up-regulated in carcinomas and mapped to chromosome 1q21, interacts with cMOAT (MRP2), the multidrug resistance-associated protein. *Lab Invest* 1999; **79**: 1161–1170.
41. Terada T, Irie M, Okuda M, Inui K. Genetic variant Arg57His in human H^+/peptide cotransporter 2 causes a complete loss of transport function. *Biochem Biophys Res Commun* 2004; **316**: 416–420.
42. Gisler SM, Pribanic S, Bacic D *et al.* PDZK1: I. A major scaffolder in brush borders of proximal tubular cells. *Kidney Int* 2003; **64**: 1733–1745.
43. Daniel H, Herget M. Cellular and molecular mechanisms of renal peptide transport. *Am J Physiol* 1997; **273**: F1–F8.
44. Wada M, Miyakawa S, Shimada A *et al.* Functional linkage of H^+/peptide transporter PEPT2 and Na^+/H^+ exchanger in primary cultures of astrocytes from mouse cerebral cortex. *Brain Res* 2005; **1044**: 33–41.
45. Cha SH, Sekine T, Fukushima J *et al.* Identification and characterization of human organic anion transporter 3 expressing predominantly in the kidney. *Mol Pharmacol* 2001; **59**: 1277–1286.
46. Sakata T, Anzai N, Shin HJ *et al.* Novel single nucleotide polymorphisms of organic cation transporter 1 (*SLC22A1*) affecting transport functions. *Biochem Biophys Res Commun* 2004; **313**: 789–793.
47. Anzai N, Deval E, Schaefer L *et al.* The multivalent PDZ domain-containing protein CIPP is a partner of acid-sensing ion channel 3 in sensory neurons. *J Biol Chem* 2002; **277**: 16655–16661.
48. Ekaratanawong S, Anzai N, Jutabha P *et al.* Human organic anion transporter 4 is a renal apical organic anion/dicarboxylate exchanger in the proximal tubules. *J Pharmacol Sci* 2004; **94**: 297–304.
49. Miyazaki H, Anzai N, Ekaratanawong S *et al.* Modulation of renal apical organic anion transporter 4 (OAT4) function by two PDZ domain-containing proteins. *J Am Soc Nephrol* 2005; **16**: 3498–3506.

A novel missense mutation of *SLC7A9* frequent in Japanese cystinuria cases affecting the C-terminus of the transporter

Y Shigeta[1,2], Y Kanai[1], A Chairoungdua[1], N Ahmed[1,2], S Sakamoto[1,2], H Matsuo[1,3], DK Kim[1,4], M Fujimura[1,2], N Anzai[1], K Mizoguchi[2], T Ueda[2], K Akakura[2], T Ichikawa[2], H Ito[2] and H Endou[1]

[1]Department of Pharmacology and Toxicology, Kyorin University School of Medicine, Shinkawa, Mitaka, Tokyo, Japan; [2]Department of Urology, Chiba University Graduate School of Medicine, Inohana, Chuo-Ku, Chiba, Japan; [3]First Department of Physiology, National Defense Medical College, , Tokorozawa, Saitama, Japan and [4]Department of Oral Physiology, Chosun University College of Dentistry, Gwangju, Korea

Cystinuria is caused by the inherited defect of apical membrane transport systems for cystine and dibasic amino acids in renal proximal tubules. Mutations in either *SLC7A9* or *SLC3A1* gene result in cystinuria. The mutations of *SLC7A9* gene have been identified mainly from Italian, Libyan Jewish, North American, and Spanish patients. In the present study, we have analyzed cystinuria cases from oriental population (mostly Japanese). Mutation analyses of *SLC7A9* and *SLC3A1* genes were performed on 41 cystinuria patients. The uptake of ^{14}C-labeled cystine in COS-7 cells was measured to determine the functional properties of mutants. The protein expression and localization were examined by Western blot and confocal laser-scanning microscopy. Among 41 patients analyzed, 35 were found to possess mutations in *SLC7A9*. The most frequent one was a novel missense mutation P482L that affects a residue near the C-terminus end of the protein and causes severe loss of function. In MDCK II and HEK293 cells, we found that P482L protein was expressed and sorted to the plasma membrane as well as wild type. The alteration of Pro^{482} with amino acids with bulky side chains reduced the transport function of $b^{0,+}$AT/BAT1. Interestingly, the mutations of *SLC7A9* for Japanese cystinuria patients are different from those reported for European and American population. The results of the present study contribute toward understanding the distribution and frequency of cystinuria-related mutations of *SLC7A9*.

Kidney International (2006) **69,** 1198–1206. doi:10.1038/sj.ki.5000241; published online 1 March 2006

KEYWORDS: cystinuria; epithelial transport; membrane transporter; proximal tubule

Correspondence: *Y Kanai, Department of Pharmacology and Toxicology, Kyorin University School of Medicine, 6-20-2 Shinkawa, Mitaka, Tokyo 181-8611, Japan. E-mail: ykanai@kyorin-u.ac.jp*

Received 29 July 2005; revised 8 October 2005; accepted 28 October 2005; published online 1 March 2006

Cystinuria (MIM 220100) is an inherited disorder owing to the defective transport of cystine and dibasic amino acids across the epithelial cells of renal proximal tubule and small intestine.[1] The incidence of cystine crystalluria reported in Western countries and in Japan varied from 15 000:1 to 50 000:1.[2,3] The patients suffer from recurrent nephrolithiasis leading to severe renal dysfunctions for which repeated therapies are imperative.[4] Classical cystinuria has been classified into three types (I, II, and III) based on the excretion of cystine and dibasic amino acids in obligate heterozygotes.[5] Type I heterozygotes show a normal amino-acid urinary pattern, whereas type II and III heterozygotes exhibit high or moderate levels of hyperexcretion of cystine and dibasic amino acids.[5] The discovery of a single-membrane-spanning type II membrane glycoprotein rBAT encoded by *SLC3A1*[6–10] and 12-membrane-spanning protein $b^{0,+}$AT/BAT1 encoded by *SLC7A9*[11–13] has brought a breakthrough in the understanding of the molecular basis of cystinuria and cystine transport in the renal proximal tubules.

The analyses of cystinuria patients have revealed distinct cystinuria-related mutations in *SLC3A1* and *SLC7A9* genes.[14,15] It was originally supposed that mutations of *SLC3A1* and *SLC7A9* genes are responsible for type I and non-type I (type II and III) cystinuria, respectively. However, recent developments in the genetics and physiology of cystinuria have not supported such a traditional classification.[16–18] Although *SLC3A1* is associated with the type I urinary phenotype, *SLC7A9* mutations were found in all three subtypes.[16,17] Therefore, a new cystinuria classification based on molecular analysis and not on urinary amino-acid excretion patterns has been proposed: type A, due to two mutations of *SLC3A1*; type B, due to two mutations of *SLC7A9*; and type AB, with one mutation on each of the above-mentioned genes.[17] For *SLC7A9* gene, International Cystinuria Consortium and Rozen and colleagues identified cystinuria-related mutations mainly from Italian, Libyan Jewish, North American, and Spanish patients

and established the genotype–phenotype relation for *SLC7A9*.[12,16–18] In the present study, we have analyzed cystinuria cases from oriental population (mostly Japanese) and found that the mutations of *SLC7A9* for Japanese cystinuria patients are quite different from those reported for European, North American, and Libyan Jewish. We report here that the most frequent one is a novel missense mutation affecting the C-terminus of the transporter protein (Tables 1 and 2).

RESULTS

Mutations of *SLC7A9* and *SLC3A1* found in cystinuria patients

We studied 41 cystinuria patients from 39 cystinuria families potentially representing 78 independent cystinuria-related alleles. They were subjected to the mutation analysis of *SLC7A9* gene by direct sequencing. The mutations of *SLC7A9* gene found in the cystinuria patients are listed in Table 3. They include one frameshift (1105delA) and one nonsense mutation (W69stop) that produce early stop codons, and seven changes affecting single amino-acid residues (V142A, G195R, L223M, N227D, R333W, R333Q, and P482L). Among them, V142A, L223M, N227D, R333Q, 1105delA, and P482L were novel mutations found for the first time in the present investigation, whereas three mutations (W69stop, G195R, and R333W) were reported previously for the European, North American, and Libyan Jewish population.[12,16,18] The amino-acid alterations except V142A and L223M were not found in 50 normal subjects. V142A and L223M were, in contrast, found in normal subjects without cystinuria phenotype. V142A and L223M were found in 23 and 19 alleles out of 50 normal subjects (100 independent alleles), respectively, suggesting that these amino-acid alterations represent polymorphic variations of *SLC7A9*.

The location of the *SLC7A9* mutations is shown at the corresponding amino-acid residues in the 12-transmembrane (TM)-domain model of $b^{0,+}$AT/BAT1 protein in Figure 1. Five cystinuria-specific missense mutations were localized within the putative TM domains 5 and 6 (G195R and N227D), in the putative intracellular loop between TM8 and TM9 (R333W and R333Q), or in the C-terminus (P482L). The one single nucleotide deletion is localized to the portion corresponding to the putative intracellular loops between TM8 and TM9 (1105delA). Three mutations (G195R, R333W, and R333Q) alter amino-acid residues that are conserved for all the human members of the heterodimeric amino-acid transporter family (Figure 1).

Among 41 cystinuria patients examined in the present study, we found mutations of *SLC3A1* in five cases. Two cases without any alterations in *SLC7A9* gene possessed mutations for *SLC3A1*: one as a homozygote for the deletion of T at nucleotide 1820; the other as a compound heterozygote for V183A (T548C)/C673R (T2017C); nucleotide numbers refer to GenBank accession no. NM_000341 for rBAT cDNA.[19] Among four cases with only polymorphic changes (V142A and/or L223M) in *SLC7A9*, two cases possessed mutations for *SLC3A1*: one as a homozygote for the insertion of TA at nucleotide 1898; the other as a compound heterozygote for V183A (T548C)/L346P (T1037C). The other two cases with only polymorphic changes in *SLC7A9* did not possess *SLC3A1* mutations. *SLC3A1* mutations were not found in the cases with cystinuria-specific mutations of *SLC7A9* except one P482L homozygote that also possesses I445T (T1334C) mutation in *SLC3A1*.

Functional analysis of *SLC7A9* mutations

All the *SLC7A9* mutations found in the present study were examined for amino-acid transport activity. As shown in Figure 2, the cystinuria-specific mutations such as W69stop, G195R, N227D, R333Q, R333W, 1105delA, and P482L exhibited remarkable decrease in cystine transport activity compared with wild-type $b^{0,+}$AT/BAT1. In contrast, V142A and L223M, which were also found in normal subjects, did not affect or only slightly decreased the cystine transport activity compared with wild-type $b^{0,+}$AT/BAT1 (Figure 2). We also constructed V142A/L223M double mutant, which contains both V142A and L223M alterations because they are possibly located in the same allele. As shown in Figure 2, even the double mutation for V142A and L223M did not severely affect the functional activity.

Table 1 | Primers used for amplification of *SLC7A9* exons and their direct sequencing

	Sense primer	Antisense primer	Size of amplified fragment
Exon 2	5′-GAGCTTGCACTTGCGTCTTG-3′	5′-AATCAAAGAGTACATCTTCTGCCG-3′	299[a]
Exon 3	5′-TGGCCTTCTGGGCTGGGTC-3′	5′-AAGAGGGATACTGGCAGGGT-3′	307
Exon 4[b]	5′-AGCCTCCGGTGGGAGGAAG-3′	5′-GAGTCCCCAGACACCCTCTG-3′	388
Exon 5[b]	5′-AAAGGAGACTCTCTCCAGGG-3′	5′-ATGCTTCCTTGGAGATGGGCT-3′	292
Exon 6	5′-CCATCTTTCCCGTGGAGATACA-3′	5′-CAAACCCCAGAAAGGAGAACTC-3′	279
Exon 7	5′-CCACTAGCAGGGCCATTCAC-3′	5′-CGGGAAGGGCATCATGGAATAC-3′	316
Exon 8[b]	5′-CTGAACGTGGGTCTCCGTG-3′	5′-ACCTCCAGTGCTGACACCTG-3′	235
Exon 9	5′-CTCTTGGAGGCCGAGAAAGAC-3′	5′-GGGTGTTATTGCTTTCGCCGC-3′	214
Exon 10	5′-TGGTCTGCACTCTGGTCAGC-3′	5′-GGCATCTGGGTCATTTGGAAG-3	236
Exon 11	5′-CTTCTTCGGTCTTCTGTGAC-3′	5′-CTAGAAGGCATGCCCCTAGC-3′	314
Exon 12	5′-AGGGGGTACATGGAGTTCATAC-3′	5′-GTGACAGAGGTCTTGGAGTC-3′	366
Exon 13	5′-CAGGGTCTAGGTGACGCATC-3′	5′-TCAGCTGACTTGGCTACAAGAG-3′	218

[a]The size of the fragments amplified by PCR using sense and antisense primers described is indicated (bp).
[b]The primers for exons 4, 5, and 8 are identical to those for reference International Cystinuria Consortium.[12]

Table 2 | The mutagenic oligonucleotide primers[a]

SLC7A9 mutagenesis primers	
W69stop	5′-CCTGCCTCATCATAT(A)[b]GGCGGCTTGCGGGG-3′
G195R	5′-CATCATCATCATCAGC(A)GGCTGGTGCTCCTGGC-3′
V142A	5′-GTGCGCCCTTCTATG(C)GGGCTGCAAGCCTC-3′
L223M	5′-GGGAGCCATCAGC(A)TGGCGTTTTACAATGG-3′
N227D	5′-CCTGGCGTTTTAC(G)ATGGACTCTGGGCC-3′
R333Q	5′-CATTTACGTGGCGGGC(A)GGGAGGGTCACATG-3′
R333W	5′-CATTTACGTGGCGGGC(T)GGGAGGGTCACATG-3′
1105delA	5′-GGGTCACATGCTCAAA*GTGCTTTCTTAC-3′
P482L	5-GGAAGTGGTCCCAC(T)GGAGGAAGACCC-3
Alanine mutagenesis primers	
M477A	5′-GCACCTTCAGATGCTA(GC)GGAAGTGGTCCCAC-3′
E478A	5′-CTTCAGATGCTAATGG(CC)GTGGTCCCACCGGA-3′
V479A	5′-CAGATGCTAATGGAAG(CG)GTCCCACCGGAGGA-3′
V480A	5′-ATGCTAATGGAAGTGG(C)CCCACCGGAGGAAGA-3′
P481A	5′-GCTAATGGAAGTGGTC(G)CACCGGAGGAAGACC-3′
E483A	5′-GAAGTGGTCCCACCGG(CT)GAAGACCCTGAGTA-3′
E484A	5′-GTGGTCCCACCGGAGG(C)AGACCCTGAGTAACA-3′
D485A	5′-GTCCCACCGGAGGAAG(C)CCCTGAGTAACAAGC-3′
P486A	5′-CCCACCGGAGGAAGAC(G)CTGAGTAACAAGCTC-3′
E487A	5′-CCGGAGGAAGACCCTG(C)GTAACAAGCTCCGTC-3′,
Leucine mutagenesis primers	
M477L	5′-CTTCAGATGCTA(C)TGGAAGTGGTCCC-3′
E478L	5″-CGAATGCTAATG(CT)AGTGGTCCCACC-3′
V479L	5-GATGCTAATGGAA(C)TGGTCCCACCGGAG-3′
V480L	5′-CTAATGGAAGTG(C)TCCCACCGGAGGA-3′
P481L	5′-ATGGAAGTGGTC(C)TACCGGAGGAAGAC-3′
E483L	5′-GTGGTCCCACCG(CT)GGAAGACCCTGAG-3′
E484L	5′-GGTCCCACCGGAG(CT)AGACCCTGAGTAAC-3′
D485L	5′-CCACCGGAGGAA(CT)CCCTGAGTAACA-3′
P486L	5′-CCAGTAGGAAGACC(T)TGAGTAACAAGCTC-3′
E487L	5′-GGAGGAAGACCCT(CT)GTAACAAGCTCC-3′
P482X mutation primers	
P482G	5′-GGAAGTGGTGCCA(GG)GGAGGAAGACCCTG-3′
P482A	5′-GGAAGTGGTCCCA(G)CGGAGGAAGACCCTG-3′
P482S	5′-GGAAGTGGTCCCA(T)CGGAGGAAGACCCTG-3′
P482V	5′-GGAAGTGGTCCCA(GT)GGAGGAAGACCCTG-3′
P482I	5′-GGAAGTGGTCCCA(ATT)GAGGAAGACCCTG-3′
P482M	5′-GGAAGTGGTCCCA(AT)GGAGGAAGACCCTG-S[1]
P482F	5′-GGAAGTGGTCCCA(TTC)GAGGAAGACCCTG-3′
P482W	5′-GGAAGTGGTCCCA(TG)GGAGGAAGACCCTG-3′

[a]Sense strand primers are shown.
[b]Mutated nucleotides are shown in parentheses.
*One nucleotide has been deleted.

P482L mutation

Among 41 cystinuria patients examined, cystinuria-specific mutations of *SLC7A9* excluding apparently polymorphic changes (V142A and L223M) were found in 35 cases (Table 3). It is noted that 25 cases were P482L homozygotes and six cases were heterozygotes involving P482L mutations. Urinary excretion levels of cystine and basic amino acids in the P482L homozygotes, compound heterozygotes involving P482L mutations, and P482L obligate heterozygotes who exhibited no cystinuria symptoms are provided in Table 4. P482L homozygotes and compound heterozygotes exhibited a high level of urinary excretion of cystine, lysine, arginine, and ornithine, whereas P482L obligate heterozygotes exhibited a significantly lower level of excretion of these amino acids, which is still higher than the normal levels (Table 4).

We further examined two family pedigrees with P482L mutation (Figure 3). In Family 1, the proband 1-6 with a clinical history of nephrolithiasis was homozygous for P482L and showed a high level of excretion of cystine and dibasic amino acids (Table 5). The heterozygotes 1-2 and 1-3 showed a lower level of amino acid excretion (Table 5). The urinary amino acid excretion of 1-1 and 1-5 without P482L mutation was within the normal range. In Family 2, 2-3 and 2-5 were homozygous for P482L, which showed a high level of urinary amino acid excretion. Although 2-2 exhibited a relatively high urinary excretion level for a heterozygote, she did not have an episode of delivery or removal of cystine stones.

Protein characterization of $b^{0,+}$AT/BAT1 mutants

We performed Western blot analyses using an antibody raised against the C-terminus portion of human $b^{0,+}$AT/BAT1 on the crude membrane fractions prepared from COS-7 cells coexpressing wild-type or mutant $b^{0,+}$AT/BAT1 with rBAT. The antibody recognized a 41 kDa protein for wild-type $b^{0,+}$AT/BAT1 in the Western blot (Figure 4a). The band disappeared in the presence of antigen peptides in the absorption experiment, confirming the specificity of immunoreactions (data not shown). As shown in Figure 4a, the bands with the identical size were detected for G195R, N227D, R333W, and R333Q mutants. The anti-C-terminus antibody could not detect W69stop and 1105delA, which lack the C-terminus portions. Furthermore, the antibody could not detect P482L, which has a mutation in the C-terminus region for which the antibody was generated (Figure 4a).

We further performed Western blot analyses using an anti-myc antibody on the membrane fractions prepared from COS-7 cells coexpressing myc-tagged wild-type or mutated $b^{0,+}$AT/BAT1 with rBAT. The anti-myc antibody recognized the bands with identical size as those detected by the anti-$b^{0,+}$AT/BAT1 C-terminus antibody (Figure 4b). The rank order of the relative band intensity of myc fusion proteins for G195R, N227D, R333W, and R333Q mutants determined by the anti-myc antibody was identical to that of G195R, N227D, R333W, and R333Q detected by the anti-C-terminus antibody. The anti-myc antibody did not detect the protein products of W69stop (~7 kDa) and 1105delA (~38 kDa) with a myc epitope on their N-termini. In contrast to the anti-C-terminus antibody, the anti-myc antibody recognized the P482L with a myc epitope on its N-terminus (myc-P482L), indicating that myc-P482L is present almost in the same amount as that for wild-type $b^{0,+}$AT/BAT1 (Figure 4b).

Localization of wild-type and P482L proteins in polarized MDCK II cells

In order to determine the subcellular localization of P482L protein, we performed confocal fluorescence analysis on the MDCK II cells expressing GFP-$b^{0,+}$AT/BAT1 (GFP: green fluorescent protein) alone or both myc-rBAT and GFP-$b^{0,+}$AT/BAT1 or GFP-P482L. For the coexpression experiments, the cells positive for both GFP fluorescence and Alexa Fluor fluorescence (myc-rBAT positive) were used for the

Table 3 | Summary of $b^{0,+}$AT/BAT1 mutations in cystinuria patients

Mutation type	Status	Nucleotide change	Exon	Protein domain	Urinary cystine (nmol/mg Cr)	Number of patients
P482L	Homozygote	C1533T	13	C-terminus	2065.8±305.3[a]	25
P482L	Heterozygote	C1533T	13	C-terminus	ND	3
P482L	Compound heterozygote	G671A	5	TM5		
G195R		C1533T	13	C-terminus	2103.5	1
P482L	Compound heterozygote	C1085T	10	IL4		
R333W		C1533T	13	C-terminus	2628.4	1
P482L	Compound heterozygote	G1086A	10	IL4		
R333Q		C1533T	13	C-terminus	ND	1
R333Q	Homozygote	G1086A	10	IL4	ND	1
N227D	Heterozygote	A767G	6	TM6	ND	1
1105delA[b]	Homozygote	1105delA	10	IL4	2118.0	1
W69stop	Compound heterozygote	G294A		TM2		
1105delA[b]		1105delA	3	IL4	ND	1
V142A	Heterozygote[c]	T513C	4	EL2		
L223M		C755A	6	TM6	ND	4
Total						39

[a]Mean±s.e.m. (n=7).
[b]1105delA results in the frameshift after Val^{340}.
[c]It is not known whether V142A and L223M mutations of these patients are in the same alleles or not.
ND, urinary cystine level was not determined for these cases. Instead, urinary cystine excretion was confirmed by cyanide-nitroprusside test. Cystine stones were also confirmed by infrared spectrophotometry.

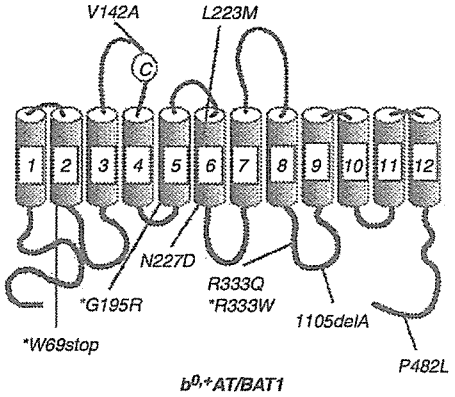

Figure 1 | Schematic representation of the mutations found in *SLC7A9* gene of patients with cystinuria. Nine mutations in *SLC7A9* gene found in 41 cystinuria patients are depicted at the corresponding amino acid residues in the 12-TM-domain model of $b^{0,+}$AT/BAT1 protein.[26] Seven mutations (W69stop, G195R, N227D, R333W, R333Q, 1105delA, and P482L) were cystinuria-specific, whereas two (V142A and L223M) were also found in the normal subjects (see text). W69stop, G195R, and N227D are located within the putative TM domains. R333Q, R333W, 1105delA, and P482L are located in the proposed intracellular loops or in the C-terminus intracellular domain. The mutations reported previously[12,16,18] were labeled with *.

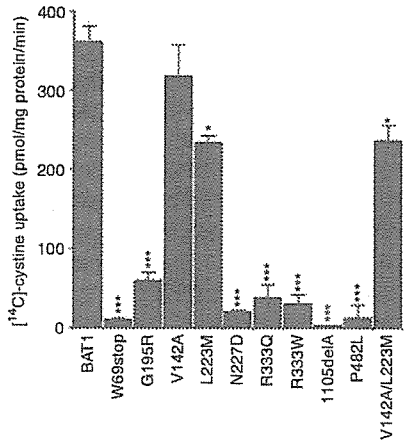

Figure 2 | Effects of *SLC7A9* mutations on the cystine transport activity. Wild-type $b^{0,+}$AT/BAT1 and indicated mutants were transiently expressed in COS-7 cells together with rBAT. The uptake of [^{14}C]L-cystine (100 μM) mediated by the expressed proteins was measured as described in 'Materials and Methods'. All transport values except those for V142A were significantly lower than those for wild-type coexpressed with rBAT. The transport values for L223M and V142A/L223M were higher than those for W69stop, G195R, N227D, R333Q, R333W, 1105delA, or P482L. V142A/L223M is a mutant that contains both V142A and L223M mutations. Asterisks indicate statistical significance (*$P<0.05$; ***$P<0.005$, Student's unpaired t-test).

analyses. As shown in Figure 5a, GFP-$b^{0,+}$AT/BAT1 protein was localized in the cytoplasm when expressed alone in MDCK II cells. Coexpression of GFP-$b^{0,+}$AT/BAT1 with myc-rBAT resulted in the apical localization of GFP-$b^{0,+}$AT/BAT1 protein in the MDCK II cells (Figure 5b). Similarly, GFP-P482L protein was also localized to the apical membrane when coexpressed with myc-rBAT (Figure 5c).

The plasma membrane expression of $b^{0,+}$AT/BAT1 and P482L proteins was further confirmed by surface biotinylation analysis (Figure 5d). HEK293 cells were used in this experiment for their higher efficiency in biotinylation analysis, probably due to the higher expression of the proteins. Consistent with the observation in COS-7 cells, myc-$b^{0,+}$AT/BAT1 but not myc-P482L showed

Table 4 | Urine amino acid levels in P482L homozygotes, compound heterozygotes, and obligate heterozygotes

		n	Cystine	Lysine	Arginine	Ornithine
P482L/P482L	Homozygotes	7	2065.8±305.3[a] (965.9–3056.6)[b]	8270.9±1185.3 (3866.8–11860.7)	3299.3±349.9 (1729.3–4482.8)	2233.0±383 (1032.1–4150.2)
R333W+P482L	Compound heterozygotes	1	2628.4	8855.4	3407.1	1592.7
G195R+P482L	Compound heterozygotes	1	2103.5	12911.5	6396.8	3744.5
P482L/+	Obligate heterozygotes	7	603.0±174.7[a, **] (56.3–1417.8)[b]	2534.7±623.5** (172.7–4781.8)	75.7±13.8** (25.6–118.4)	170.9±62.0** (18.2–354.5)
	Normal range		20–150	50–1300	10–60	5–40 (nmol/mg creatinine)

[a]Mean±s.e.m. (n=7).
[b]Range of amino acid excretion levels.
**P<0.01, versus homozygotes and compound heterozygotes (Mann–Whitney U-test).

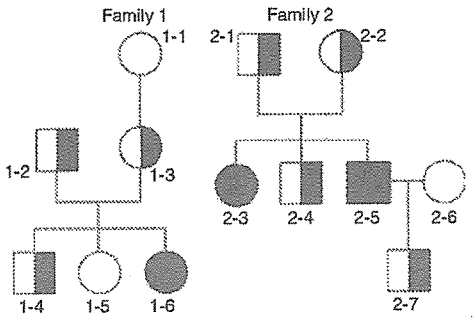

Figure 3 | Pedigrees of Japanese cystinuria families with P482L mutation. Two Japanese families (Families 1 and 2) with P482L mutation examined are shown.

Table 5 | Urinary excretion levels of cystine and dibasic amino acids of two family pedigrees

Individual no.[a]	Cystine	Lysine	Arginine	Ornithine	Sum
1-1	32.8	102.9	193.7	51.9	381.3
1-2	160.3	904.2	22.5	21	1108
1-3	791.1	3164.1	107.9	328.8	4391.9
1-4	385	2912.5	61.6	60.5	3419.6
1-5	64.7	222.8	23.1	20.1	330.7
1-6[b]	2240	7049	3538.3	2026.1	14853.4
2-1	255.6	1062.4	33.6	42.7	1394.3
2-2	1417.8	4012.9	100.3	354.5	5885.5
2-3	2932.6	9726.3	3440.7	2364.4	18464
2-4	ND	ND	ND	ND	ND
2-5[b]	1677.9	6370	2478.8	1692.7	12219.4
2-6	ND	ND	ND	ND	ND
2-7	891.7	4781.8	118.4	352.9	6144.8
Normal range	20–150	50–1300	10–60	5–40	(nmol/mg creatinine)

[a]The individual numbers are corresponded to those of members of the family pedigrees shown in Figure 4.
[b]1-6 and 2-5 are probands.
ND, Not determined.

[^{14}C]L-cystine uptake when coexpressed with rBAT in HEK293 cells (data not shown). As shown in Figure 5d, myc-$b^{0,+}$AT/BAT1 and myc-P482L proteins were detected at the plasma membrane when coexpressed with rBAT. The myc-$b^{0,+}$AT/BAT1 and myc-P482L proteins were not detected at plasma membrane when solely expressed (Figure 5d).

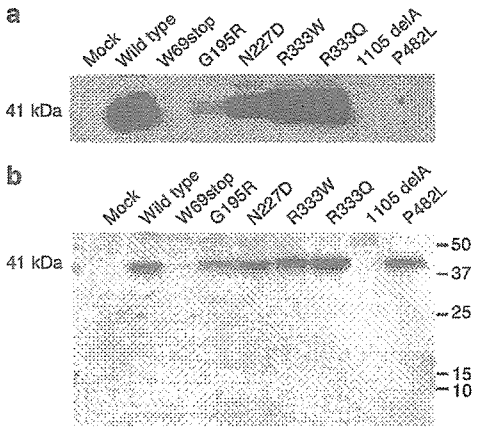

Figure 4 | Western blot analysis of $b^{0,+}$AT/BAT1 and its mutants. (a) $b^{0,+}$AT/BAT1 and its mutants were transiently expressed in COS-7 cells with rBAT. The Western blot analysis using an anti-$b^{0,+}$AT/BAT1 C-terminus antibody was performed on the membrane fraction prepared from the COS-7 cells. The anti-$b^{0,+}$AT/BAT1 C-terminus antibody recognized a 41 kDa band for wild-type $b^{0,+}$AT/BAT1 and its mutants except W69stop, 1105delA, and P482L. (b) An anti-myc antibody was used to detect $b^{0,+}$AT/BAT1 and its mutants to which a myc epitope was added at their N-termini. The myc-tagged proteins were transiently expressed in COS-7 cells with rBAT. In the Western blot, the anti-myc antibody recognized a 41 kDa band for wild-type $b^{0,+}$AT/BAT1 and its mutants including P482L.

Effect of P482L mutation

In order to understand why P482L, a single amino acid alteration at the C-terminus of the transporter protein, resulted in the loss of transport function, we performed site-directed mutagenesis analyses. For the series of mutants in which residues between Met^{477} and Glu^{487} were systematically changed to alanine, no remarkable decrease was observed in the [^{14}C]L-cystine transport activity compared with wild-type $b^{0,+}$AT/BAT1 (Figure 6a). It is notable that the alteration of Pro^{482} to alanine did not affect the [^{14}C]L-cystine transport activity in contrast to the severe decrease in the transport activity observed for P482L. We, then, changed individual amino acid residues located between residues 477 and 487 to leucine (Figure 6b). We found that P481L, V479L, M477L, E478L, and V480L, in addition to P482L, exhibited a significant decease in the [^{14}C]L-cystine transport activity

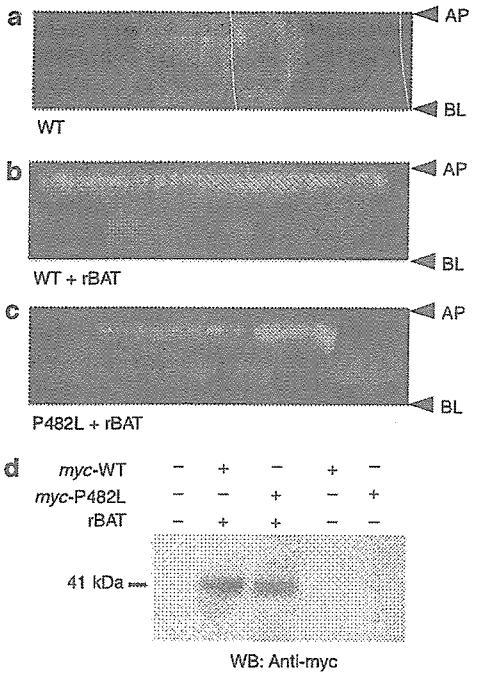

Figure 5 | Localization of P482L protein on the plasma membrane. Shown are the *x–z* images of confocal laser-scanning microscopic analyses on the MDCK II cells expressing (**a**) GFP-$b^{0,+}$AT/BAT1, (**b**) GFP-$b^{0,+}$AT/BAT1 with rBAT, and (**c**) GFP-P482L with rBAT. GFP-$b^{0,+}$AT/BAT1 and GFP-P482L fusion proteins were sorted to the apical membrane of the MDCK II cells when coexpressed with rBAT. In contrast, GFP-$b^{0,+}$AT/BAT1 fusion protein stayed in the cytoplasm when solely expressed. AP and BL indicate apical and basal sites of MDCK II cells, respectively. (**d**) Cell surface biotinylation analysis of $b^{0,+}$AT/BAT1 and P482L. HEK293 cells were transiently expressed with myc-$b^{0,+}$AT/BAT1 plus rBAT (lane 2), myc-P482L plus rBAT (lane 3), myc-$b^{0,+}$AT/BAT1 alone (lane 4), or myc-P482L alone (lane 5). Single bands of ~41 kDa were observed for myc-$b^{0,+}$AT/BAT1 and myc-P482L coexpressed with rBAT (lane 2 and 3). Green: GFP fluorescence; red: 4,6-diamidino-2-phenylindole fluorescence from nuclei.

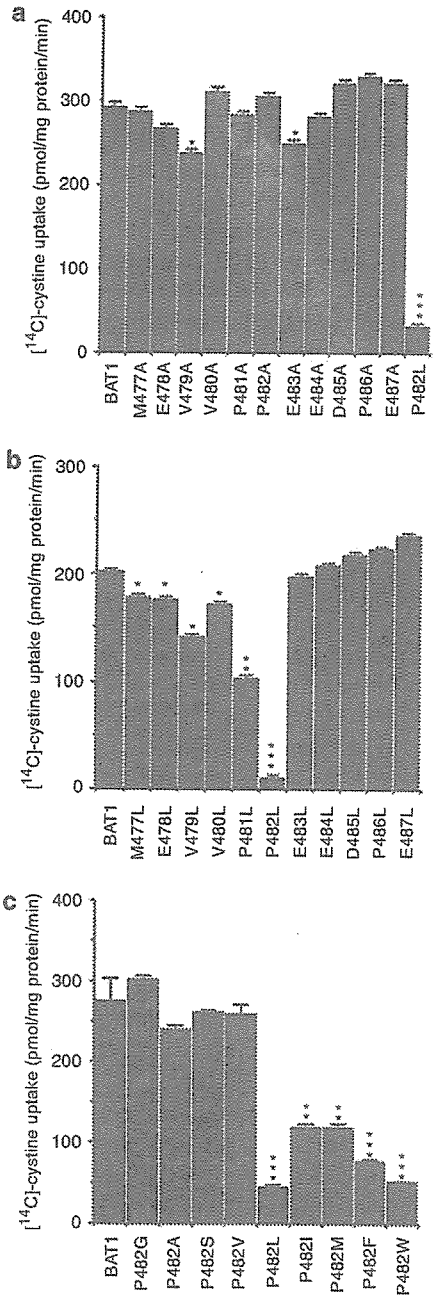

Figure 6 | Effects of site-directed mutagenesis of C-terminus of $b^{0,+}$AT/BAT1 on [^{14}C]L-cystine uptake. (**a**) The C-terminus amino acids between residues 477 and 487 of $b^{0,+}$AT/BAT1 were systematically mutated to alanine. The site-directed mutants exhibited no remarkable decrease in the uptake of [^{14}C]L-cystine compared with that of wild type except for P482L mutation. (**b**) The C-terminus amino acids between residues 477 and 487 of $b^{0,+}$AT/BAT1 were systematically mutated to leucine. When Pro^{482} was changed to leucine, the mutants expressed with rBAT exhibited remarkable decrease in the uptake of [^{14}C]L-cystine (100 μM). (**c**) Pro^{482} of $b^{0,+}$AT/BAT1 was mutated to amino acids with varied bulkiness in their side chains. The alteration of Pro^{482} to leucine, isoleucine, methionine, phenylalanine, and tryptophan remarkably decreased the transport activity, whereas the alteration to glycine, alanine, serine, and valine did not change the transport activity. Asterisks indicate statistical significance (*$P<0.05$; **$P<0.01$; ***$P<0.005$, Student's unpaired *t*-test).

compared with wild-type $b^{0,+}$AT/BAT1; however, the magnitude of the decrease was much less than that for P482L. In order to further investigate the effect of the alteration of Pro^{482} to Leu, we constructed mutants in which Pro^{482} is changed to various neutral amino acids with varied bulkiness in their side chains. As shown in Figure 6c, the alteration of Pro^{482} to amino acids with bulky side chains such as leucine, isoleucine, methionine, phenylalanine, and tryptophan severely decreased the [^{14}C]L-cystine transport activity, whereas the change to the amino acids with less-bulky side chains such as glycine, alanine, serine, and valine did not affect the functional activity.

DISCUSSION

In the present study, we examined cystinuria patients from oriental population (40 Japanese and one Korean) and found that mutations of *SLC7A9* gene responsible for the disease of the oriental population are quite different from those reported previously for European, North American, and

Libyan Jewish.[12,16,18] In contrast to W69Stop, G195R, and R333W reported previously,[12,16,18] N227D, R333Q, 1105delA, and P482L found in the present study are novel cystinuria-specific mutations, suggesting that these mutations are unique to Japanese or Asian. It is noted that 31 out of 35 cases with cystinuria-specific mutations examined in the present study involved P482L mutation, whereas this mutation has not been reported for European, North American, and Libyan Jewish population.[12,16,18] It is, therefore, supposed that P482L mutation is prevailing in Japanese and possibly in the other Asian population. G105R, the most frequent mutation for European, North American, and Libyan Jewish population (~25% of non-type I cystinuria cases),[18] was not found in the present study. It is interesting that two cystinuria-specific missense mutations R333Q and R333W found in the present study affect the same amino acid residue, in which R333Q was only found for Japanese cases. Arg^{333} is located in the putative intracellular loop between TM domains 8 and 9 and conserved for human members of heterodimeric amino acid transporter family.[18] It is, thus, proposed that this amino acid residue is critical in the transport function or in the structural framework for the light chains of heterodimeric amino acid transporters.

For P482L mutation most abundantly found in the present study, we examined two family pedigrees and confirmed Mendelian inheritance and phenotype–genotype correlation (Figure 3 and Table 5). The homozygotes of this mutation exhibited severe cystinuria phenotype with episodes of excretion or removal of renal stones and high level of urinary excretion of cystine and dibasic amino acids. Compared with normal individuals, P482L heterozygotes exhibited a higher level of excretion of cystine and dibasic amino acids into urine, consistent with the characteristics of non-type I cystinuria (Table 5). Relatively large range of variation in the amount of urinary excretion was observed among heterozygotes (2-1, 2-2, and 2-7). This might be due to the possible genetic alterations of $b^{0,+}$AT/BAT1 or rBAT that could not be detected in the present study, variations in other factors related to the transporter systems, or differences in diet and metabolism. We found three P482L heterozygotes who suffer from nephrolithiasis. For these patients, no mutation was found in the exons of *SLC3A1* gene encoding rBAT. Although we cannot exclude the involvement of additional mutations of *cis*-regulatory elements of *SLC7A9* gene and *SLC3A1* gene or the mutations of unidentified genes that might be essential for cystine transport, P482L heterozygous mutation could possibly cause cystinuria symptoms dependent on the condition of the patients, which has been reported for classic type II cystinuria with severe phenotypes.[16,20]

P482L is the missense mutation affecting the C-terminus of $b^{0,+}$AT/BAT1. As shown in Figure 2, this mutation results in the loss of function of $b^{0,+}$AT/BAT1 protein coexpressed with rBAT in COS-7 cells, indicating that Pro^{482} plays pivotal role in the functional expression of the transporter. Loss of function of P482L mutant is supposed not due to the loss of protein expression or lack of ability to be sorted to the apical membrane based on the following reasons: first, the anti-myc antibody recognized the band for myc-tagged P482L with the intensity similar to that of wild-type $b^{0,+}$AT/BAT1 (Figure 4b); second, the GFP-tagged P482L protein was sorted to the apical membrane when coexpressed with rBAT in MDCK II cells similar to GFP-tagged wild-type $b^{0,+}$AT/BAT1 (Figure 5b and c); finally, surface biotinylation study revealed that P482L protein as well as wild-type $b^{0,+}$AT/BAT1 protein was detected at the plasma membrane upon coexpression with rBAT in HEK293 cells (Figure 5d). In Figure 4b, the protein products of W69stop and del1105A were not detected. This might be due to the rapid degradation of the immature proteins. A recent study on the crystal structure of *Escherichia coli* 12-membrane-spanning transporters indicated that the substrate binding sites are located in the hydrophilic pocket surrounded by TM helices, suggesting that their N- and C-terminal intracellular domains are not directly involved in the substrate binding and translocation of substrates.[21,22] Mammalian 12-membrane-spanning transporters phylogenetically related to the bacterial 12-membrane-spanning transporters are supposed to possess the analogous structure and operate based on the similar structural trait.[23] In order to examine the roles of Pro^{482} in the C-terminus intracellular domain of $b^{0,+}$AT/BAT1, we performed site-directed mutagenesis analyses. In the first series of experiments, C-terminus amino-acid residues between Met^{477} and Glu^{487} were systematically changed to alanine. Surprisingly, no remarkable decrease was observed in the cystine transport activity even when Pro^{482} was changed to alanine in spite of the severe decrease in the function for Pro^{482}-to-Leu alteration. This indicates that Pro^{482} itself is not essential for the function of $b^{0,+}$AT/BAT1 protein but the incorporation of leucine residue at position 482 interferes with the functional expression.

We, thus, generated additional site-directed mutants in which Pro^{482} was changed to various neutral amino acids. As shown in Figure 6, the alteration of Pro^{482} to amino acids with bulky side chains affected the function of $b^{0,+}$AT/BAT1, whereas the changes to residues with less bulky side chains did not reduce the functional activity. It is, thus, suggested that the bulky side chains incorporated at the C-terminus of $b^{0,+}$AT/BAT1 interfered with the functional expression of $b^{0,+}$AT/BAT1. By examining the site-directed mutants in which residues between Met^{477} and Glu^{487} were systematically changed to leucine, it was found that leucine alteration affected the function of $b^{0,+}$AT/BAT1 only when quite restricted residues were changed to leucine. Based on these observations, we, thus, propose that the bulky side chain incorporated at the position 482 of $b^{0,+}$AT/BAT1 somehow suppressed the transport function possibly by interfering with intra- or intermolecular interactions. The further investigation would lead to the understanding of the novel regulatory mechanisms of heterodimeric amino acid transporters as well as the role of P482L mutation in the pathogenesis of cystinuria.

In the present study, we have identified several novel mutations of *SLC7A9* from oriental population and found that mutations are quite different from those reported previously for European, North American, and Libyan Jewish. Our results contribute toward understanding the distribution and frequencies of cystinuria-related mutations of *SLC7A9*.

MATERIALS AND METHODS

Subjects

Forty-one cystinuria patients (40 Japanese and one Korean) from 39 independent families were studied. All had an episode of delivery or removal of cystine stones. Urinary excretion of cystine and dibasic amino acids was determined in 24 h urine samples by quantitative ion-exchange chromatography or reverse-phase high-performance liquid chromatography. The amino acid content was corrected per gram of creatinine. In all patients whose urinary cystine excretion was analyzed quantitatively, cystine excretion was over 800 nmol/mg creatinine. Urinary hyperexcretion of dibasic amino acids was also confirmed. The urinary excretion of other neutral amino acids was within normal ranges for all patients. For the patients whose urinary amino acid levels were not quantitatively analyzed, the urinary cystine excretion was confirmed by cyanide-nitroprusside test and their cystine stones were analyzed by infrared spectrophotometry.[3] Genomic DNA was obtained from the patients and the members of the selected family pedigrees. Genomic DNA was also obtained from 50 unrelated normal individuals who served as controls. The study protocol was approved by the Institutional Research Boards of Chiba University Graduate School of Medicine and of Kyorin University School of Medicine. All study subjects gave written informed consent, and the ethics committee of Chiba University Graduate School of Medicine and of Kyorin University School of Medicine gave permission for the analyses in relation to cystinuria.

Determination of *exon–intron* boundaries of *SLC7A9*

The location and sequence of all exon–intron boundaries were determined by direct sequencing of the products obtained by PCR amplification of genomic DNA with randomly designed cDNA-derived oligonucleotide primers, using an ABI PRISM Sequencer (Perkin Elmer, Wellesley, MA, USA). *SLC7A9* consisted of 13 exons. The codon for the translation-initiator methionine (ATG) was located in exon 2, whereas the termination codon TAA was located in exon 13. The exon–intron boundaries we determined have turned out to be identical to those obtained by deducing the recently released genomic DNA sequence of *SLC7A9* (accession no. AC008805).[18]

Mutation analysis and direct sequencing

Genomic DNA was extracted from whole blood using the Wizard Genomic DNA Purification Kit (Promega, Madison, WI, USA). Twelve pairs of oligonucleotide primers (Table 1) were synthesized in order to amplify all exons of *SLC7A9* gene by PCR for direct sequencing. In all cases, sequencing of both strands of the PCR products was performed.[24] Mutation analysis of *SLC3A1* gene was performed for the above-described 41 cystinuria patients using oligonucleotide primers as described elsewhere.[25]

Construction of mutant cDNAs

All cDNA mutants were constructed by using the QuikChange site-directed mutagenesis kit (Stratagene, La Jolla, CA, USA) according to the manufacturer's instructions. The mutagenic oligonucleotide primers are shown in Table 2. Proper construction of the mutated cDNAs was confirmed by complete sequencing.

Functional expression in COS-7 cells

cDNAs for human rBAT and those for wild-type or mutated human $b^{0,+}$AT/BAT1 in pcDNA3.1(+) were expressed transiently in COS-7 cells using LipofectAMINE™2000 (Invitrogen, Carlsbad, CA, USA) following the manufacturer's instructions.[26] For co-transfection, 10 μg of cDNA for $b^{0,+}$AT/BAT1 or its mutants and 10 μg of rBAT cDNA were diluted into 1 ml of opti-MEM reduced-serum medium (Invitrogen, Carlsbad, CA, USA) and mixed with 60 μl LF2000 reagent diluted in 1 ml opti-MEM reduced-serum medium. After incubation for 20 min at room temperature, the mixture was applied to COS-7 cells maintained in a tissue culture dish (90 mm diameter) with 70–90% confluence. At 24 h after transfection, the transfected cells were collected and seeded on a 24-well plate (2×10^5 cells/well) in fresh medium. Amino acid uptake measurements were performed at 48 h after transfection of the plasmids as described elsewhere.[26]

Anti-human $b^{0,+}$AT/BAT1 antibodies

Oligopeptides (QMLMEVVPPEEDPEC) corresponding to amino acid residues 474–487 of human $b^{0,+}$AT/BAT1 were synthesized. Anti-peptide antibody was produced as described elsewhere.[27,28]

Construction of the fusion proteins

The fusion proteins in which myc and GFP epitopes were fused to the N-terminus of wild-type and mutant $b^{0,+}$AT/BAT1 were generated. The coding regions of cDNAs for the wild-type and mutant $b^{0,+}$AT/BAT1 were amplified by PCR using primers containing restriction enzyme cleavage sites for *Hin*dIII, *Xho*I, *Eco*RI, or *Kpn*I. After digestion with *Hin*dIII and *Xho*I or *Eco*RI and *Kpn*I, the fragments were ligated with pCMV-Taq3 vector (Stratagene, La Jolla, CA, USA) digested with *Hin*dIII and *Xho*I or pEGFP C2 vector (Clontech, Mountain View, CA, USA) digested with *Eco*RI and *Kpn*I, respectively. Proper construction was confirmed by DNA sequencing.

Western blotting

COS-7 cells were co-transfected with cDNAs for human rBAT and those for wild-type, mutated human $b^{0,+}$AT/BAT1 or their myc-tagged products as described above. At 48 h after transfection, the transfected cells were collected and homogenized as described elsewhere.[29] The anti-human $b^{0,+}$AT/BAT1 (1:2000) antibody or anti-myc (1:2000) antibody (Invitrogen, Carlsbad, CA, USA) was used as the primary antibody. To verify the specificity of immunoreactions by absorption experiments, the membranes were treated with primary antibodies in the presence of antigen peptides (50 μg/ml).[29]

Confocal laser-scanning microscopy

MDCK II cells provided by Dr Dietrich Keppler (European Molecular Biology Laboratory, Heidelberg, Germany) were cultured as described.[30] For localization of $b^{0,+}$AT/BAT1 and P482L mutant protein, MDCK II cells were grown on transwell membranes (membrane diameter 24 mm, pore size 3.0 μm; Costar, Corning, NY, USA) for 1 week (100% confluence) and then co-transfected with cDNAs for myc-tagged human rBAT (1 μg) and those for GFP-tagged wild-type human $b^{0,+}$AT/BAT1 or GFP-P482L (1 μg) using LipofectAMINE™2000. Cells were fixed with 4% paraformaldehyde in phosphate-buffered saline and permeabilized with 0.5% Triton X-100 in phosphate-buffered saline containing 5% goat serum.

Membranes were incubated with an anti-myc (1:500) antibody (Invitrogen, Carlsbad, CA, USA) at room temperature for 1 h. After three washes with phosphate-buffered saline, the membranes were incubated with Alexa Fluor 546 goat anti-mouse IgG (Molecular Probes, Eugene, OR, USA) as a secondary antibody for 1 h. Argon and HeNe laser beams were used for excitation at 488 nm for GFP and 543 nm for Alexa Fluor 546 visualization, respectively. Nuclei were stained with 4,6-diamidino-2-phenylindole nucleic acid staining for 10 min and visualized by excitation at 405 nm with Diode 405 laser. Images were acquired using Carl Zeiss LSM510 META laser-scanning confocal microscope (Carl Zeiss, Frankfurt, Germany).

Cell surface biotinylation

Surface biotinylation of $b^{0,+}$AT/BAT1 and P482L mutant at the plasma membrane of HEK293 cells was performed as describe elsewhere.[31,32] myc-tagged $b^{0,+}$AT/BAT1 and myc-P482L were detected with an anti-myc (1:2000) antibody (Invitrogen) and horseradish peroxidase-conjugated anti-mouse IgG as a secondary antibody (Jackson ImmunoResearch, West Grove, PA, USA).

Statistical analysis

Data are expressed as mean $\pm$ s.e.m. Statistical differences were determined using Student's unpaired *t*-test. Mann–Whitney *U*-test was used to analyze urinary amino-acid levels among different genotypes. Differences were considered significant at the level of $P<0.05$.

ACKNOWLEDGMENTS

This work was supported in part by grants from the Ministry of Education, Culture, Sports, Science and Technology of Japan, the Japan Society for the Promotion of Science, the Promotion and Mutual Aid Corporation for Private Schools of Japan, the Japan Health Sciences Foundation, Uehara Memorial Foundation, YASUDA Medical Research Foundation, Heiwa Nakajima Foundation, and Health and Labor Sciences Research Grants for Research on Advanced Medical Technology: Toxicogenomics Project. AC is a research fellow of the Japan Society for Promotion of Science. We thank Dr K Nozumi, Dr T Yoshida, Dr T Igarashi, Dr K Yamaguchi, Dr H Suniya, Dr K Nagashima, Dr M Masai, Dr H Nakatsu, Dr S Tomioka, Dr K Mikami, Dr Y Naya, and Dr K Egoshi for help with obtaining blood samples. We also thank Michi Takahashi, Akie Toki, and Keiko Sakama for technical assistance. Anti-$b^{0,+}$AT/BAT1 antibody was supplied by Kumamoto Immunochemical Laboratory, Transgenic Inc., Kumamoto, Japan.

REFERENCES

1. McKusick VA. Cystiuria. In: *Mendelian Inheritance in Man: Catalog of Autosomal Dominant, Autosomal Recessive, and X-linked Phenotypes*, 9th edn. Johns Hopkins University Press: Baltimore and London, 1990, pp 1128–1129.
2. Segal S, Thier SO. Cystiuria. In: Seriver CR, Beaudet AL, Sly WS, Valle D (eds). *The Molecular and Metabolic Basis of Inherited Disease*. McGraw-Hill: New York, 1995, pp 3581–3601.
3. Ito H, Murakami M, Miyauchi T *et al.* The incidence of cystinuria in Japan. *J Urol* 1982; **129**: 1012–1014.
4. Akakura K, Egoshi K, Ueda T *et al.* The long-term outcome of cystinuria in Japan. *Urol Int* 1998; **61**: 86–89.
5. Rosenberg L, Downing S, Durant J, Segal S. Cystinuria biochemical evidence of three genetically distinct diseases. *J Clin Invest* 1966; **45**: 365–371.
6. Wells RG, Hediger MA. Cloning of a rat kidney cDNA that stimulates dibasic and neutral amino acid transport and has sequence similarity to glucosidases. *Proc Natl Acad Sci USA* 1992; **89**: 5596–5600.
7. Bertran J, Werner A, Moore ML *et al.* Expression cloning of a cDNA from rabbit kidney cortex that induces a single transport system for cystine and dibasic and neutral amino acids. *Proc Natl Acad Sci USA* 1992; **89**: 5601–5605.
8. Tate SS, Yan N, Udenfriend S. Expression cloning of a Na^+-independent neutral amino acid transporter from rat kidney. *Proc Natl Acad Sci USA* 1992; **89**: 1–5.
9. Lee WS, Wells RG, Sabbag RV *et al.* Cloning and chromosomal localization of a human kidney cDNA involved in cystine, dibasic and neutral amino acid transport. *J Clin Invest* 1993; **91**: 1959–1963.
10. Bertran J, Werner A, Chillaron J *et al.* Expression cloning of a human renal cDNA that induces high affinity transport of L-cystine shared with dibasic amino acids in *Xenopus* oocytes. *J Biol Chem* 1993; **268**: 14842–14849.
11. Chairoungdua A, Segawa H, Kim JY *et al.* Identification of an amino acid transporter associated with the cystinuria-related type II membrane glycoprotein. *J Biol Chem* 1999; **274**: 28845–28848.
12. International Cystinuria Consortium. Non-type I cystinuria caused by mutations in *SLC7A9*, encoding a subunit ($b^{0,+}$AT) of rBAT. *Nat Genet* 1999; **23**: 52–57.
13. Pfeiffer R, Loffing J, Rossier G *et al.* Luminal heterodimeric amino acid transporter defective in cystinuria. *Mol Biol Cell* 1999; **10**: 4135–4147.
14. Palacin M, Fernandez E, Chillaron J, Zorzano A. The amino acid transport system $b^{0,+}$ and cystinuria. *Mol Membr Biol* 2001; **18**: 21–26.
15. Palacin M, Borsani G, Sebastio G. The molecular bases of cystinuria and lysinuric protein intolerance. *Curr Opin Genet Dev* 2001; **11**: 328–335.
16. Leclerc D, Boutros M, Suh D *et al.* SLC7A9 mutations in all three cystinuria subtypes. *Kidney Int* 2002; **62**: 1550–1559.
17. Dello Strologo L, Pras E, Pontesilli C *et al.* Comparison between *SLC3A1* and *SLC7A9* cystinuria patients and carriers: a need for a new classification. *J Am Soc Nephrol* 2002; **13**: 2547–2553.
18. Font MA, Feliubadalo L, Estivill X *et al.* Functional analysis of mutations in *SLC7A9*, and genotype–phenotype correlation in non-Type I cystinuria. *Hum Mol Genet* 2001; **10**: 305–316.
19. Calonge MJ, Gasparini P, Chillaron J *et al.* Cystinuria caused by mutations in rBAT gene involved in the transport of cystine. *Nat Genet* 1994; **6**: 420–425.
20. Goodyer P, Saadi I, Ong P *et al.* Cystinuria subtype and the risk of nephrolithiasis. *Kidney Int* 1998; **54**: 56–61.
21. Abramson J, Smirnova I, Kasho V *et al.* Structure and mechanism of the lactose permease of *Escherichia coli*. *Science* 2003; **301**: 610–615.
22. Huang Y, Lemieux MJ, Song J *et al.* Structure and mechanism of the glycerol-3-phosphate transporter from *Escherichia coli*. *Science* 2003; **301**: 616–620.
23. Locher KP, Bass RB, Rees DC. Structural biology. Breaching the barrier. *Science* 2003; **301**: 603–604.
24. Enomoto A, Kimura H, Chairoungdua A *et al.* Molecular identification of a renal urate anion exchanger that regulates blood urate levels. *Nature* 2002; **417**: 447–452.
25. Egoshi K, Akakura K, Kodama T, Ito H. Identification of five novel *SLC3A1* (rBAT) gene mutations in Japanese cystinuria. *Kidney Int* 2000; **57**: 25–32.
26. Mizoguchi K, Cha SH, Chairoungdua A *et al.* Human cystinuria-related transporter: localization and functional characterization. *Kidney Int* 2001; **59**: 1821–1833.
27. Altman A, Cardenas JM, Houghten RA *et al.* Antibodies of predetermined specificity against chemically synthesized peptides of human interleukin 2. *Proc Natl Acad Sci USA* 1984; **81**: 2176–2180.
28. Hisano S, Haga H, Miyamoto K *et al.* The basic amino acid transporter (rBAT)-like immunoreactivity in paraventricular and supraoptic magnocellular neurons of the rat hypothalamus. *Brain Res* 1996; **710**: 299–302.
29. Yanagida O, Kanai Y, Chairoungdua A *et al.* Human L-type amino acid transporter 1 (LAT1): characterization of function and expression in tumor cell lines. *Biochim Biophys Acta* 2001; **1514**: 291–302.
30. Cui Y, Konig J, Buchholz JK *et al.* Drug resistance and ATP-dependent conjugate transport mediated by the apical multidrug resistance protein, MRP2, permanently expressed in human and canine cells. *Mol Pharmacol* 1999; **55**: 929–937.
31. Anzai N, Miyazaki H, Noshiro R *et al.* The multivalent PDZ domain-containing protein PDZK1 regulates transport activity of renal urate-anion exchanger URAT1 via its C terminus. *J Biol Chem* 2004; **279**: 45942–45950.
32. Huh KH, Wenthold RJ. Turnover analysis of glutamate receptors identifies a rapidly degraded pool of the *N*-methyl-D-aspartate receptor subunit, NR1, in cultured cerebellar granule cells. *J Biol Chem* 1999; **274**: 151–157.

Available online at www.sciencedirect.com
SCIENCE DIRECT
Toxicology and Applied Pharmacology 210 (2006) 200–211
Toxicology and Applied Pharmacology
www.elsevier.com/locate/ytaap

Prenatal 3,3′,4,4′,5-pentachlorobiphenyl exposure modulates induction of rat hepatic CYP 1A1, 1B1, and AhR by 7,12-dimethylbenz[*a*]anthracene

Shin Wakui[a,*], Kiyofumi Yokoo[a], Hiroyuki Takahashi[b], Tomoko Muto[c], Yoshihiko Suzuki[d], Yoshikatsu Kanai[c], Hiroshi Hano[b], Masakuni Furusato[e], Hitoshi Endou[c]

[a]*Department of Toxicologic Pathology, Azabu University School of Veterinary Medicine, 1-17-71 Fuchinobe, Kanagawa 229-8501, Japan*
[b]*Department of Pathology, The Jikei University School of Medicine, Tokyo 105-8461, Japan*
[c]*Department of Pharmacology and Toxicology, Kyorin University School of Medicine, Tokyo 181-8611, Japan*
[d]*Department of Biochemistry, Azabu University School of Veterinary Medicine, Kanagawa 229-8501, Japan*
[e]*Department of Pathology, Kyorin University School of Medicine, Tokyo 181-8611, Japan*

Received 8 February 2005; accepted 30 April 2005
Available online 28 June 2005

Abstract

We previously reported the finding that prenatal exposure to a relatively low dose of PCB126 increases the rate of DMBA-induced rat mammary carcinoma, while a high dose decreased it. One of the most important factors determining the sensitivity to mammary carcinogenesis is the metabolic stage at administration of the carcinogenic agent. DMBA is a procarcinogen that recruits the host metabolism to yield its ultimate carcinogenic form, and CYP1A1 and CYP1B1 (CYP1) conduct this metabolism. We investigated the hepatic expression of CYP1 and AhR following oral administration of DMBA (100 mg/kg b.w.) (i.g.) to 50-day-old female Sprague–Dawley rats whose dams had been treated (i.g.) with 2.5 ng, 250 ng, 7.5 μg of PCB126/kg or the vehicle on days 13 to 19 post-conception. Real-time quantitative RT-PCR analysis revealed that the prenatal exposure to a relatively low dose of PCB126 (the 250 ng group) prolonged the higher expression of CYP1A1, CYP1B1, and AhR mRNA, while prenatal exposure to a high dose of PCB126 (the 7.5 μg group) prolonged the higher expression of CYP1A1 and AhR mRNA. Western blotting and immunohistochemical analyses were consistent with mRNAs changes. Because DMBA oxidation produces a highly mutagenic metabolite and is finally catalyzed by CYP1B1, a relatively low PCB126 dose might produce the biological character to potentially increase the risk of DMBA-induced mammary carcinoma.

Keywords: PCB126; DMBA; CYP1; AhR; Liver; Rat

Introduction

Polychlorinated biphenyls (PCBs) are a heterogeneous group of man-made organic compounds that are widely present in the environment (IARC, 1997). The chemical stability and lipophilicity of PCBs and their resistance to degradation results in their persistence and concentration in food chains (Bro-Rasmussen, 1996) as well as their bioaccumulation in human adipose tissue (Kutz et al., 1991), blood (Murphy and Harvey, 1985), and breast milk (Rogan et al., 1987). Moreover, transplacental and lactational transfers of PCBs to a developing fetus and infant have the potential to cause adverse effects (Safe and Krishnan, 1995; van den Berg et al., 1998).

7,12-Dimethylbenz[*a*]anthracene (DMBA) is a model compound that induces mammary carcinogenesis in rodents (Huggins et al., 1961; MacDonald et al., 2001; Rowlands et

Abbreviations: PCBs, polychlorinated biphenyls; CYP, cytochrome P450; AhR, aryl hydrocarbon receptor; ARNT, AhR nuclear translocator protein; PCB126, 3,3′,4,4′,5-pentachlorobiphenyl; DMBA, 7,12-dimethylbenz[*a*]anthracene.

* Corresponding author. Fax: +81 42 754 7661.
E-mail address: wakui@azabu-u.ac.jp (S. Wakui).

0041-008X/$ - see front matter © 2005 Elsevier Inc. All rights reserved.
doi:10.1016/j.taap.2005.04.022

al., 2001). We previously found that prenatal exposure to a relatively low dose of 3,3′,4,4′,5-pentachlorobiphenyl (PCB126) increases rat mammary carcinoma induced by DMBA ingestion at 50 days old, and exposure to a high dose of PCB126 acts as an inhibiting agent for it (Muto et al., 2001). One of the most important factors determining sensitivity to mammary carcinogenesis is the metabolic stage of the carcinogenic agent. DMBA is a procarcinogen and requires metabolic conversion to its ultimate carcinogenic metabolite by oxidation, which is conducted by CYP1A1 and 1B1 (CYP1) (Christou et al., 1987; Dipple, 1995; Shimada et al., 1996). Both the proximate and ultimate metabolites of DMBA that are formed in hepatocytes can be transported to other organs, resulting in carcinogen-adducted DNA (Di Giovanni and Juchau, 1980; Ginsberg and Atherholt, 1989). Therefore, the liver has a primary role in the metabolism of DMBA and is the most significantly affected organ following the experimental exposure of DMBA to an animal (Di Giovanni and Juchau, 1980; Kothari and Subramanian, 1992). Thus, the extent to which DNA adducts occur after administration of DMBA depends on the level of oxidative metabolism of DMBA due to CYP1 activities (Dipple et al., 1999; Granberg et al., 2000; MacDonald et al., 2001; Rowlands et al., 2001).

Both PCB126, a prototypical coplanar halogenated aromatic hydrocarbon, and DMBA, a polycyclic aromatic hydrocarbon, bind and activate the aryl hydrocarbon receptor (AhR), which is a basic helix–loop–helix (b-HLH) protein (Burback et al., 1992). Ligand binding results in activation of AhR and subsequent nuclear translocation, where it heterodimerizes with another bHLH partner, the AhR nuclear translocator protein (ARNT) (Hoffman et al., 1991). The AhR–ARNT dimer binds to specific regulatory elements, xenobiotic responsive elements (XREs), upstream of the responsive genes and enhances their transcripts, the CYP1 enzyme family (Dolwick et al., 1993; Jones et al., 1986; Okey et al., 1994; Rowlands et al., 2001; Schmidt and Bradfield, 1996). Enzyme activation of carcinogens yields intermediate metabolites that are chemically more reactive than the initial compound (Cavalieri et al., 2002). Hence, we investigated the expressions of hepatic CYP1 and AhR following ingestion of DMBA by 50-day-old offspring of female rats that had been exposed to PCB126 on days 13 to 19 post-conception.

Materials and methods

Animals, chemicals, and treatments. Forty-five female and nine male 6-week-old Sprague–Dawley (slc) rats (Japan SLC, Shizuoka, Japan) were housed, three per plastic cage, on hardwood-chip bedding in an environment-controlled room on a 12-h light/12-h dark cycle at 22 ± 2 °C and 55% ± 5% relative humidity, with a conventional diet (MF, Oriental Yeast, Tokyo, Japan). All experimental procedures were conducted following approval of the Animal Care and Use Committee of the Azabu University School of Veterinary Medicine. Guidelines set by the National Institute of Health and Public Health Service Policy on the Humane Use and Care of Laboratory Animals were followed at all times. PCB126 was obtained from AccuStandard Inc., New Haven, CT, and DMBA was obtained from Tokyo Chemical Industry Co. Ltd., Tokyo, Japan. Seven-week-old rats were housed with five females and a male per plastic cage.

A lifetime tolerable daily intake (TDI) of PCB126 has been reported to range from 10 to 100 pg/kg/day (van den Berg et al., 1998). In this study, three doses of PCB126 were selected using 25 pg/kg/day as the TDI dose (Muto et al., 2001): 10^2-fold of the TDI dose, 10^4-fold of the TDI dose, and 3×10^5-fold of the TDI dose. Groups of eight pregnant rats were treated with 2.5 ng, 250 ng, or 7.5 μg/kg body (i.g.) PCB126 or with an equivalent volume of corn oil (~0.5 ml/animal, i.g.), on days 13 through 19 post-conception. The offspring were sexed at birth, and litters were reduced so that each dam was left with eight offspring (four females/dam). Weaning was carried out at day 21 post-partum. In this study, we considered the group of rats with prenatal exposure to 2.5 ng, 250 ng, or 7.5 μg/kg body PCB126 or with an equivalent volume of corn oil as the 2.5-ng, the 250-ng, the 7.5-μg, or the vehicle group, respectively.

Each PCB126-treated group (2.5-ng, 250-ng, or 7.5-μg group) included forty-five females, and the vehicle group included thirty-six females. For experiments, 135 fifty-day-old female rats received 100 mg/kg DMBA in corn oil/kg body (i.g.), and 36 received an equivalent volume of corn oil (~0.5 ml/animal, i.g.). In this study, the dose of DMBA was selected following the study of Huggins et al. (1961) with the conversion using animal body weight. Following anesthesia by diethyl ether, liver samples were obtained under deep anesthesia from five (DMBA-fed) and four (corn oil-fed) rats from each group at 6 h, 12 h, 1 day, 2 days, 5 days, 10 days, 20 days, and 30 days. Representative sections of each liver were fixed in 10% phosphate-buffered formalin and routinely processed for immunohistochemistry. In addition, representative sections were frozen without fixation and stored at −80 °C.

Chemical analysis. Analysis for PCB126 was carried out following the alkaline alcohol digestion method (Tanabe et al., 1987). Aliquots of homogenized rat mammary tumor samples were refluxed in 1 N KOH–ethanol solution for 1 h. The PCB126 thus extracted into ethanol was transferred to 100 ml of hexane by shaking in a separating funnel. Subsequently, the hexane layer was concentrated and purified by passing it through 1.5 g of silica gel (Wako gel S-1, Wako Co., Ltd., Osaka, Japan) packed in a glass column (10 mm inside diameter × 200 mm length). PCB126 was eluted with 200 ml of hexane at an elution rate of one drop per second. The eluate was concentrated to 5 ml in a Kuderna–Danish concentrator and further purified with 5% fuming sulphuric acid. All samples were injected into a gas chromatograph-mass spectrometer (GC-MS: Shimadzu 9020

DF with an SCAP-1123 data system, Shimadzu Co. Ltd., Kyoto, Japan) equipped with an electron-impact ion-source and moving needle-type injection system for the determination and identification of PCB126. The column consisted of a 0.23 mm I.D. × 30 m glass capillary, coated with silicone. Operating conditions of the GC-MS were as follows: column oven temperature was programmed to rise from 190 °C to 250 °C at 0.5 °C min^{-1}; injector and ion-source temperatures were kept at 250 °C and 280 °C, respectively. PCB126 was determined by selected ion monitoring at *m/z* 326. The carrier flow of helium was controlled at 0.6 ml min^{-1}.

Immunohistochemistry. Immunohistochemical expressions of CYP1A1 and CYP1B1 were analyzed using the avidin–biotin complex (ABC) method. After deparaffinization, 4 μm thick sections were treated sequentially with 0.3% H_2O_2 for 10 min, then blocked with 10% goat serum or horse serum in PBS for 20 min. Sections were thawed, rinsed in PBS, and treated with primary antibodies of rabbit anti-rat-CYP1A1 (Affiniti Res. Inc., Exeter, UK; diluted 1:1000) and rabbit anti-CYP1B1 (BD Biosciences, Bedford, MA; diluted 1:50). Bound IgG was detected with biotinylated goat anti-rabbit IgG (Vector Lab., Burlingame, CA; diluted 1:100) followed by avidin–biotin complex (ABC)-peroxidase (Vector Lab., Burlingame, CA) and diaminobenzidine (Sigma, St. Louis, MO). Sections were then counterstained with hematoxylin. As a negative control, non-immunized rabbit serum was substituted for the primary antibody.

Real-time quantitative RT-PCR. For each RNA sample, 100 ng was used as the template for first strand cDNA synthesis using a TaqMan Reverse Transcription kit, following the RT-PCR manufacturer's two-step protocol (PE Applied Biosystems, Foster City, CA). Controls included for each reaction were the RNA sample without reverse transcriptase (RNA − RT) and no RNA with reverse transcriptase (no RNA + RT). The conditions of the final reaction for reverse-transcription were as follows: 1 × TaqMan RT buffer; 5.5 mM $MgCl_2$; 500 μM dATP, dGTP, and dCTP; 1 mM dTTP; Random Hexamers 0.25 μM; 1.25 Ul MuLV reverse transcriptase and 0.4 U RNase inhibitor (PE Applied Biosystems, Foster City, CA). Quantitative analyses of target gene (CYP1A1, CYP1B1, and AhR) mRNA expression were performed by real-time quantitative PCR using the ABI Prism 7700 Sequence Detection System (PE Biosystems, Foster City, CA) with Taq Man chemistry and probe. The TaqMan probes and primers for target genes were assay-on-demand gene expression products (PE Applied Biosystems, Foster City, CA) and oligonucleotides with fluorescent reporter and quencher dyes attached (Table 1). Optimal primer, probe, and cDNA concentrations were determined in a separate set of experiments to insure that both target gene and GAPDH fragments were amplified with equal efficiency. PCR reactions were performed with first-strand cDNA synthesis (2 μl) from each sample, a Universal PCR Master Mix kit (PE Applied Biosystems, Foster City, CA), 250 nM TaqMan probe, 0.16 U of AmpErase UNG (uracil N-glycosylase), and 900 nM forward-reverse primers of the target gene and GAPDH. Three measurements per sample were performed in each of two independent experiments. Results were analyzed with the ABI Sequence Detector software version 1.7 (PE Applied Biosystems, Foster City, CA). For relative quantification of target gene expression, the standard curve method was applied. The calibrated standard curve of each target gene cDNA and GAPDH amplification plots were examined at five different dilutions (containing 100, 50, 25, 10, or 5 ng) of total RNA samples that were obtained from each PCR product using a TOPO II TA Cloning Kit (Invitrogen, Carlsbad, CA) following the manufacturer's recommendations. The target gene's normalized value was determined by dividing the average target gene value by the average GAPDH value. The standard deviation (SD) of the quotient is calculated from the SD of the target gene and GAPDH using the following formula:

$$CV = (\text{SD of the quotient})/(\text{mean value of the quotient})$$

$$(CV)^2 = (CV_1)^2 + (CV_2)^2$$

$$CV_1 = (\text{SD of target gene value})/(\text{mean of target gene value})$$

$$CV_2 = (\text{SD of GAPDH value})/(\text{mean of GAPDH value})$$

The normalized target gene value is a unitless number that can be used to compare the relative amount of the target gene in different samples. One way to make this comparison is to designate one of the samples as a calibrator. In this study, the liver of 50-day-old rat of the vehicle group without DMBA ingestion was designated as the calibrator, and the averaged target gene value was divided by the average calibrator value according to the manufacturer's instructions for quantification of relative gene expression (User Bulletin #2; P/N 4303859, pp. 3–30, 36).

Western blot analysis. Rat livers were homogenized in 50 mM Tris–HCl, 150 mM KCl (pH 7.4), 1% Triton X-100, and 0.25 mM phenylmethylsulfonyl fluoride (PMSF) and centrifuged at 8000 × *g* for 30 min at 4 °C. The supernatant obtained was centrifuged at 100,000 × *g* for 90 min at 4 °C.

Table 1
ID numbers of TaqMan probes and primers (Assay-on-Demand gene expression products) used for real-time quantitative RT-PCR

Gene	ID
CYP1A1	Rn0048721_m1
CYP1B1	Rn00564055_m1
AhR	Rn00565750_m1

Assay-on-Demand gene expression products were supplied by PE Applied Biosystems, Foster City, CA.

Table 2
Body and liver weights of 50-day-old female rats after prenatal PCB126 exposure

Group	Body weight (mg)	Liver weight (mg)
7.5 μg	242.25 ± 4.07	12.06 ± 0.89
250 ng	245.32 ± 4.21	12.22 ± 0.53
2.5 ng	243.26 ± 5.82	11.70 ± 0.55
Vehicle	243.22 ± 6.22	11.86 ± 0.76

Values represent mean ± SEM Scheffé's F test, NS.

The pellet was suspended in 50 mM Tris–HCl (pH 7.4), 1% Triton X-100, and 1 mM PMSF, and the protein concentrations were determined with a bicinchonic acid protein assay reagent kit (Pierce, Rockford, IL) with bovine serum albumin as a standard. Microsomal samples were subjected to electrophoresis on a 10% SDS polyacrylamide gel using 10 μg of microsomes. The proteins were transferred for 2 h to a nitrocellulose membrane that was blocked by immersing it in 5% non-fat dried milk in phosphate-buffered saline with 0.1% (v/v) Tween 20 (PBS-T). Western blot analysis was performed using anti-rat-CYP1A1 (Affiniti Res., Exeter, UK), anti-rat-CYP1B1 (BD Gentest, San Jose, CA), or anti-AhR (H-211) (Santa Cruz, Santa Cruz, CA) antibodies. CYP1A1, CYP1B1, and AhR antibodies were diluted 1:1000, 1:500, and 1:1000, respectively, in PBS-T and incubated 1 h at room temperature on an orbital shaker. After being washed three times with PBS-T, they were incubated with a 1:2500 dilution of horseradish peroxidase-conjugated anti-rabbit antibody (Amersham Biosciences, Piscataway, NJ) for 1 h on an orbital shaker. After being washed three times with PBS-T, the membranes were detected using the ECL Plus Western Blotting Detection System (Amersham Biosciences, Piscataway, NJ).

Statistical analysis. For each set, the mean value, standard deviation, and standard error of the mean were calculated and compared using Scheffé's F test or a chi-square test using the computer statistical analysis system Stat View-J 5.0 (Abacus Concepts, Cary, NC).

Results

Body and liver weights, and concentration of PCB126 in liver

Prenatal PCB126 treatment of dams resulted in offspring with body weights and liver weights that were similar between groups at 50 days old (Table 2). The concentration of PCB126 in the liver of 50-day-old rats compared to the vehicle group was about 365 times higher in the 7.5-μg group, about 12 times higher in the 250 ng group, and about 1.5 times higher in the 2.5 ng group, and that of 80-day-old rats compared to the vehicle group was about 26 times higher in the 7.5-μg group, about 1.4 times higher in the 250-ng group, and about 1.1 times higher in the 2.5-ng group (Table 3).

Table 3
Concentration of PCB126 in livers of female rats after prenatal exposure

Group	50-day-old	80-day-old
7.5 μg	73.05 ± 8.68*	5.01 ± 3.79
250 ng	2.35 ± 1.39	0.26 ± 0.96
2.5 ng	0.30 ± 0.98	0.21 ± 0.88
Vehicle	0.20 ± 0.42	0.19 ± 0.37

Values represent mean ± SEM ng/g.
* Scheffé's F test, $P < 0.05$.

Quantitative RT-PCR for CYP1A1 and CYP1B1 mRNA expression in prenatally PCB126-exposed rat liver

In 50-day-old rats, the 7.5-μg group showed significantly increased expression of hepatic CYP1A1 mRNA (33-fold) and CYP1B1 mRNA (15-fold), and the other groups showed lower expression of CYP1A1 mRNA (1- to 3-fold) and CYP1B1 mRNA (1- to 1.7-fold) (Figs. 1, 2). As they grew older, the CYP1 mRNA expression levels of the 7.5-μg group gradually decreased, but remained at significantly higher levels compared with that of the other groups until they were 70 days old (Figs. 1, 2).

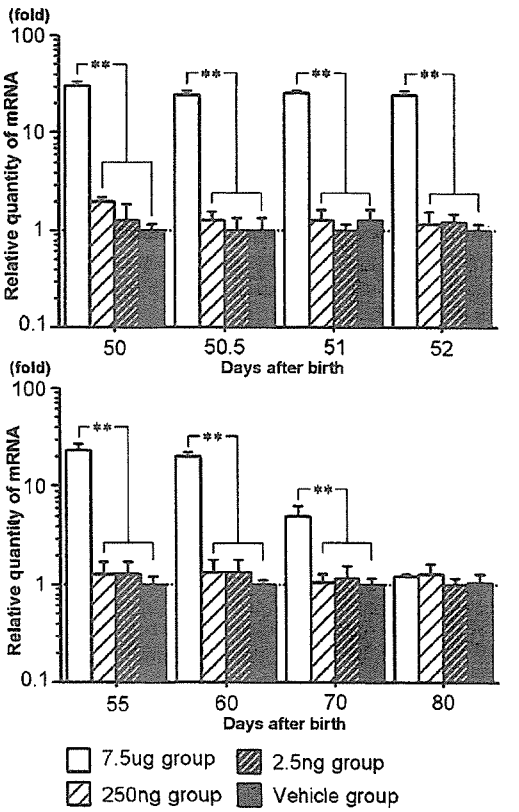

Fig. 1. Effect of prenatal exposure to PCB126 on CYP1A1 mRNA expression in rat liver. The indicated mRNA levels were determined by real-time quantitative RT-PCR, with analysis using the standard curve method described under Materials and methods. Each level was normalized to that of the endogenous housekeeping gene GAPDH in each tissue, as described under Materials and methods. Values represent mean ± SD. (**) Scheffé's F test $P < 0.01$.

Quantitative RT-PCR for CYP1A1mRNA expression following DMBA ingestion in prenatally PCB126-exposed rat liver

At 6 h after DMBA ingestion, the expression of CYP1A1 mRNA was significantly higher in all PCB126-treated groups (33- to 34-fold) than in the vehicle group (25-fold) (Fig. 3). After 12 h, all groups showed a similarly high level (Fig. 3). After 1 day, CYP1A1 mRNA expression of all PCB126-treated groups remained at high levels, but that of the vehicle group decreased to 25-fold (Fig. 3). After 2 days, CYP1A1 mRNA expression of the 7.5-μg and 250-ng groups remained at similarly high levels, but that of the 2.5 ng and vehicle groups decreased to 15- to 17-fold (Fig. 3). At 5 days after, CYP1A1 mRNA expression of the 7.5-μg and 250-ng groups showed a 28- to 32-fold increase, and that of 2.5-ng group had decreased 12-fold, while in the vehicle group, it had decreased to the calibrator level (Fig. 3). Subsequently, CYP1A1 mRNA expression of the 7.5-μg and 250-ng groups was gradually decreased to 22- to 28-fold at 10 days after, 18- to 20-fold at 20 days after, and CYP1A1 mRNA expression of the 2.5 ng and vehicle groups had returned to the calibrator level at 10 to 20 days after (Fig. 3). At 30 days after, CYP1A1 mRNA expression of all groups had returned to the calibrator level (Fig. 3).

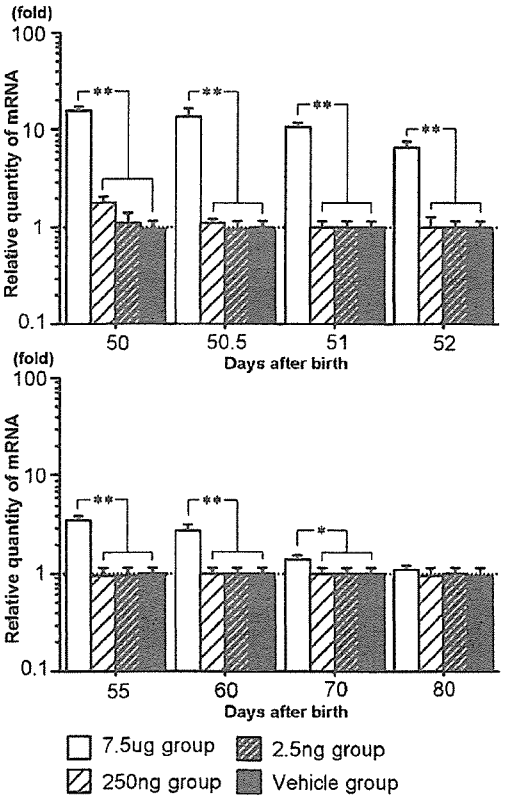

Fig. 2. Effect of prenatal exposure to PCB126 on CYP1B1 mRNA expression in rat liver. The indicated mRNA levels were determined by real-time quantitative RT-PCR, with analysis using the standard curve method described under Materials and methods. Each level was normalized to that of the endogenous housekeeping gene GAPDH in each tissue, as described under Materials and methods. Values represent mean ± SD. (**) Scheffé's F test $P < 0.01$. (*) Scheffé's F test $P < 0.05$.

Quantitative RT-PCR for CYP1B1mRNA expression following DMBA ingestion in prenatally PCB126-exposed rat liver

At 6 h after DMBA ingestion, the expression of CYP1B1 mRNA of all PCB126-treated groups had increased (24- to 26-fold), but that of the vehicle group remained at the calibrator level (Fig. 4). After 12 h to 1 day, CYP1B1 mRNA expression of the 7.5-μg and 250-ng groups increased further to 25- to 27-fold, and that of vehicle group also increased to 17- to 18-fold (Fig. 4). At 2 days after, CYP1B1 mRNA expression of the 7.5-μg and 250-ng groups remained at similarly high levels, but in the vehicle group it had decreased to 14-fold (Fig. 4). At 5 days after, CYP1B1 mRNA expression of the 250-ng group showed a 20-fold increase, which was significantly higher than that of the 7.5-μg and 2.5-ng groups (9- to 10-fold), and the vehicle group had decreased to the calibrator level (Fig. 4). After 10 to 20 days, CYP1B1 mRNA expression of the 250-ng group was 18-fold, which was significantly higher than that of the 7.5-μg group (8-fold), and the 2.5-ng and vehicle groups had returned to the calibrator level (Fig. 4). After 30 days, CYP1B1 mRNA expression of the 250-ng group was 2-fold, which was significantly higher than that of the 2.5-ng and vehicle groups (Fig. 4).

Quantitative RT-PCR for AhR mRNA expression following DMBA ingestion in prenatally PCB126-exposed rat liver

At 6 h after DMBA ingestion, the expression of AhR mRNA had increased, but those of all PCB126-treated groups (33-fold) were significantly higher than that of the vehicle group (25-fold) (Fig. 5). At 12 h after, AhR mRNA expression of all groups showed similarly high levels (Fig. 5). At 1–2 days after, AhR mRNA expression of the vehicle group gradually decreased (Fig. 5). At 5 days after, AhR mRNA expression of the 250-ng group was 35-fold, which was significantly higher than that of the 7.5-μg and 2.5-ng groups, and in the vehicle group, it had decreased to the calibrator level (Fig. 5). At 10–20 days after, AhR mRNA expression of the 250-ng group gradually decreased, but it was significantly higher than that of the 7.5-μg group, and in the 2.5-ng and vehicle groups, it was at the calibrator level (Fig. 5). After 30 days, all groups were at the calibrator level (Fig. 5).

Immunohistochemistry for CYP1A1 and CYP1B1, and Western blot analyses of CYP1A1, CYP1B1, and AhR expression following DMBA ingestion in prenatally PCB126-exposed rat liver

To determine whether the mRNA modulation of the CYP1 and AhR correlates with changes in protein expres-

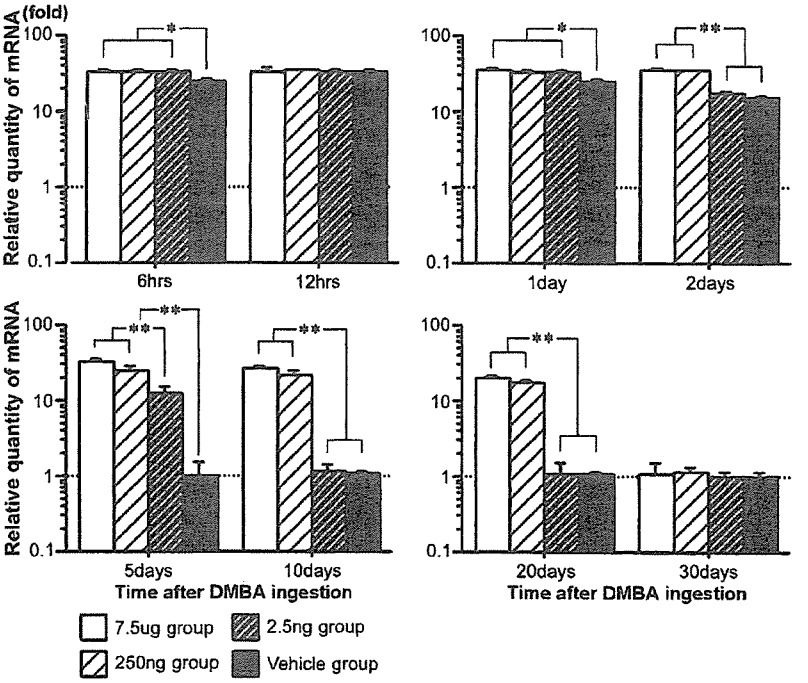

Fig. 3. Effect of prenatal exposure to PCB126 on CYP1A1 mRNA expression in rat liver following DMBA ingestion. The indicated mRNA levels were determined by real-time quantitative RT-PCR, with analysis using the standard curve method described under Materials and methods. Each level was normalized to that of the endogenous housekeeping gene GAPDH in each tissue, as described under Materials and methods. Values represent mean ± SD. (**) Scheffé's F test $P < 0.01$ (*) Scheffé's F test $P < 0.05$.

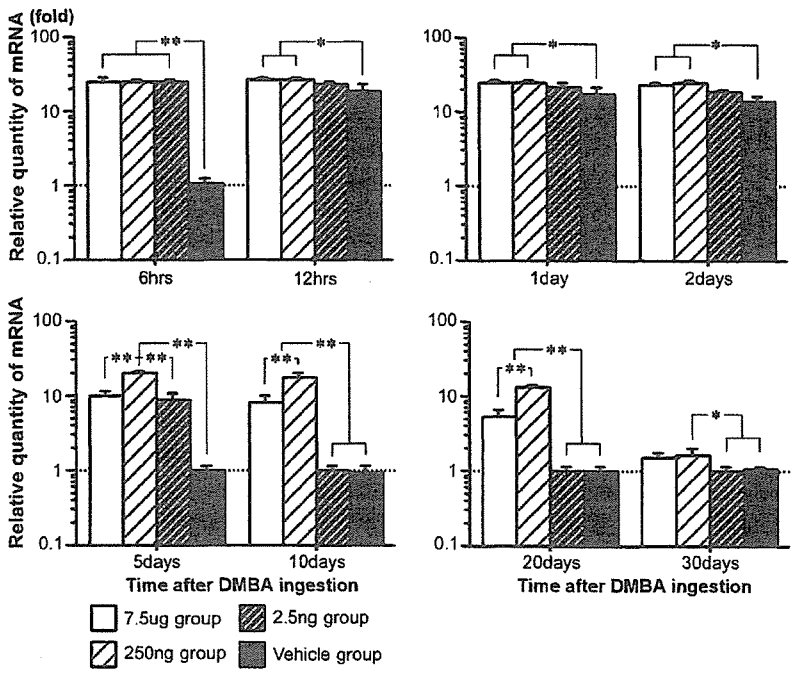

Fig. 4. Effect of prenatal exposure to PCB126 on CYP1B1 mRNA expression in rat liver following DMBA ingestion. The indicated mRNA levels were determined by real-time quantitative RT-PCR, with analysis using the standard curve method described under Materials and methods. Each level was normalized to that of the endogenous housekeeping gene GAPDH in each tissue, as described under Materials and methods. Values represent mean ± SD. (**) Scheffé's F test $P < 0.01$ (*) Scheffé's F test $P < 0.05$.

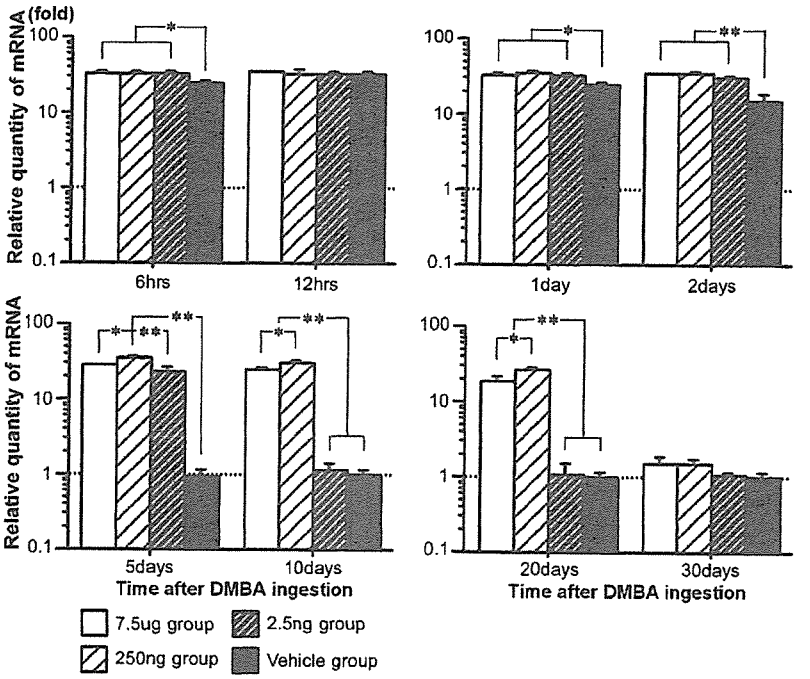

Fig. 5. Effect of prenatal exposure to PCB126 on AhR mRNA expression in rat liver following DMBA ingestion. The indicated mRNA levels were determined by real-time quantitative RT-PCR, with analysis using the standard curve method described under Materials and methods. Each level was normalized to that of the endogenous housekeeping gene control GAPDH in each tissue, as described under Materials and methods. Values represent mean ± SD. (**) Scheffé's F test $P < 0.01$ (*) Scheffé's F test $P < 0.05$.

sion, immunohistochemistry, and/or Western blot analyses were performed. The protein expression was qualitatively consistent with the patterns observed for CYP1A1 mRNA, CYP1B1 mRNA, and AhR mRNA (Figs. 6–8).

Discussion

PCBs are ubiquitous environmental contaminants that produce a spectrum of adverse biochemical and biological effects, including carcinogenic effects in people and a wide variety of animals (IARC, 1997). The induction of CYP1 expression by PCBs and DMBA has been extensively investigated (Angus et al., 1999; Christou et al., 1987; Rowlands et al., 2001; Schmidt and Bradfield, 1996; Whitlock, 1999), and it has been established that the nuclear AhR/ARNT heterodimeric complex acts as a ligand-activated transcription factor that binds to XREs in the regulatory region of CYP1 genes (Evans, 1988).

Our previous study found that rats given 250 ng PCB126/kg/day (from days 13 through 19 post-conception) had a higher incidence of DMBA-induced mammary carcinogenesis than a group given 7.5 μg PCB*126*/kg/day (from days 13 through 19 post-conception) (Muto et al., 2001). PCBs are considered non-genotoxic carcinogens because they do not produce DNA adducts and are negative for genotoxic tests (Turteltaub et al., 1990), while DMBA, a member of the polycyclic aromatic hydrocarbons (PAHs), is a procarcinogen and requires metabolic conversion to its ultimate carcinogen metabolite, DMBA-3,4-dihydrodiol-1,2-epoxide (Dipple et al., 1984; Slaga et al., 1979; Sims and Grover, 1981), by a process that includes two separate oxidations, produces 3,4-dihydrodiol, and is catalyzed by either CYP1A1 or CYP1B1 (Christou et al., 1987; Ciolino et al., 2002). The second oxidation produces the highly mutagenic 3,4-dihydrodiol-1,2-epoxide metabolite and is catalyzed by CYP1B1 (Shimada et al., 1996). These data suggest that CYP1B1 is an essential enzyme for metabolic activation, and thus the carcinogenic potential of DMBA is dependent on it. In this study, the 7.5-μg group showed higher expression of CYP1A1 until 20 days after DMBA ingestion, while the 250-ng group showed higher expression of CYP1A1 until 20 days after and higher expression of CYP1B1 until 30 days after. The mechanisms controlling the tissue-specific transcription of CYP1B1 are now not known (Sasaki et al., 2003). Our results are the first demonstration, to our knowledge, of a modulation of CYP1B1 expression by PAHs. Indeed, it has been suggested that CYP1B1 possesses a greater capacity than CYP1A1 to bioactivate a number of PAH procarcinogens (MacDonald et al., 2001; Shimada et al., 1996). Because Western blotting and immunohistochemical analyses were qualitatively consistent with each mRNA change, increased activities of these enzymes would also be revealed in the increased protein expression.

When DMBA was ingested at 50 days old, only the 7.5-μg group showed a high level of hepatic CYP1 expression, and it had decreased to that of the calibrator level at 80 days

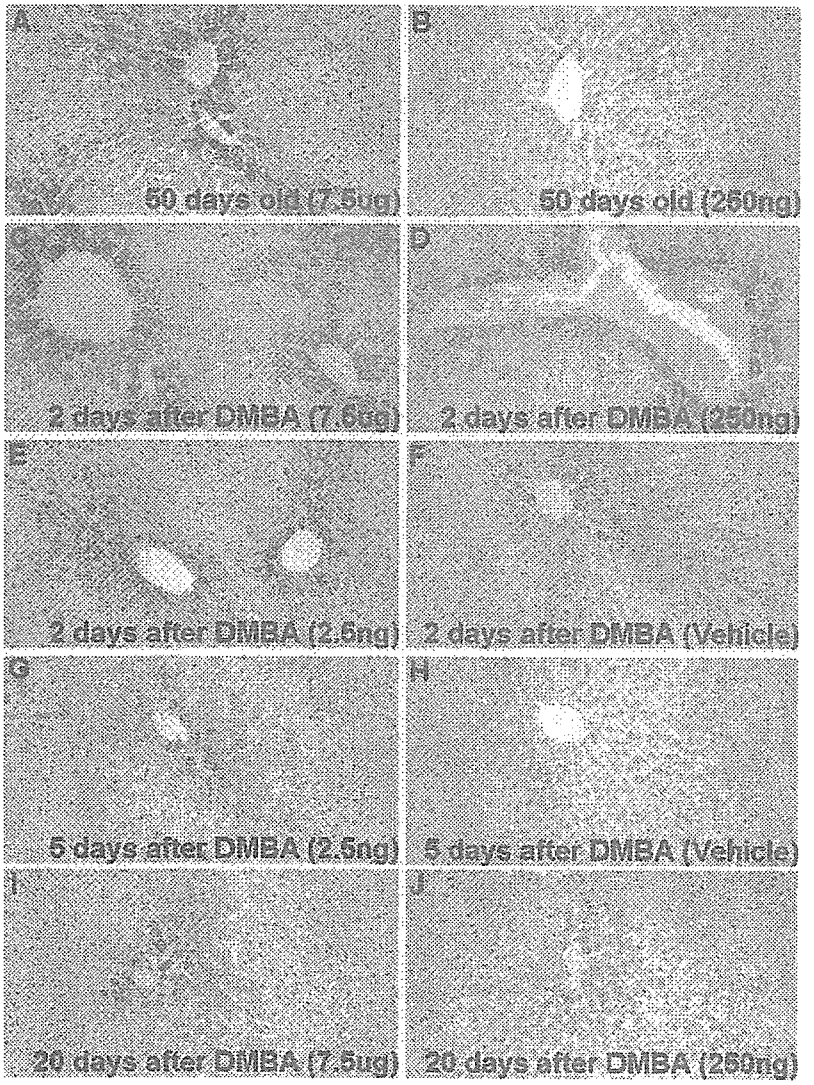

Fig. 6. Immunohistochemical analysis of CYP1A1 in rat liver. Just before DMBA ingestion, a large number of hepatocytes in the 7.5-μg group were positive (A) for CYP1A1, but negative in the 250-ng group (B). At 2 days after DMBA administration, a large number of hepatocytes were positive in the 7.5-μg (C) and 250-ng groups (D), and many hepatocytes were positive in the 2.5 ng (E) and vehicle groups (F). At 5 days after administration, some hepatocytes were positive in the 2.5-ng group (G), but none was positive in the vehicle group (H). At 20 days after DMBA administration, some hepatocytes were positive in the 7.5-μg group (I), and a few hepatocytes were positive in the 250-ng group (J). ABC method, Mayer's hematoxylin counterstain. Magnification ×140.

old. Because the 7.5-μg group possessed a high level of hepatic PCB126 residues (more than 31 times that of the other groups) on the day of DMBA ingestion, these CYP1 inductions were thought to be due to a complex induction by PCB126 residues and ingested DMBA, while the 250-ng and 2.5-ng group revealed prolonged CYP1 inductions compared to that of the vehicle group. Because the 250-ng and 2.5-ng groups showed a lower level of CYP1 with lower PCB126 residues at the time of DMBA ingestion (50 days old), it seems that prenatal exposure to PCB126 increases hepatocyte sensitivity in the rat for CYP1 induction by ingested DMBA.

The precise mechanism of the modulation of DMBA-induced mammary carcinogenesis by PCB126 remains to be explained, but one possible mechanism could be the ability of CYP1A1 and CYP1B1 to metabolize highly oxidative DMBA because carcinogenesis was dominant in the 250-ng group, while the concentration of PCB126 residues due to prenatal exposure that induced a high level of CYP1A1 was highest in the 7.5-μg group. The predominance of CYP1B1 in several human cancers, including breast carcinomas (Eltom et al., 1998; Merchant et al., 1993; Murray et al., 1997), has been reported. The functional involvement of CYP1B1 in PAH metabolism has been demonstrated by the fact that the metabolism of DMBA by microsomes from MCF-7 cells is inhibited by anti-CYP1B1 antibody, but not anti-CYP1A1 antibody (Christou et al., 1995). Although it is well known that PCBs specifically induce CYP1 (Angus et al., 1999; Christou et al., 1987; Tritscher et al., 1992), it remains to

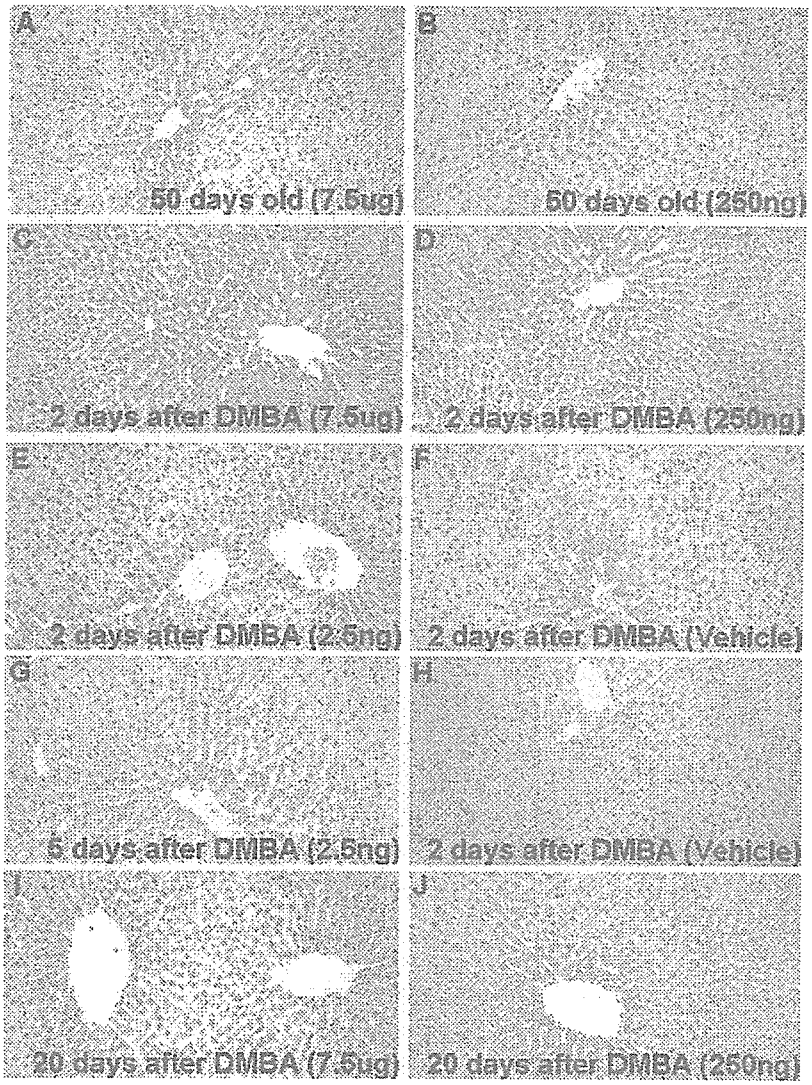

Fig. 7. Immunohistochemical analysis of CYP1B1 in rat liver. Just before DMBA ingestion, some hepatocytes in the 7.5-μg group were positive for CYP1B1 (A) but negative in the 250-ng group (B). At 2 days after DMBA administration, a large number of hepatocytes were positive in the 7.5-μg (C) and 250-ng groups (D), and many hepatocytes were positive in the 2.5 ng (E) and vehicle group (F). At 5 days after DMBA administration, some hepatocytes were positive in the 2.5 ng group (G), but none was positive in the vehicle group (H). At 20 days after DMBA administration, a few hepatocytes were positive in the 7.5-μg group (I), and some hepatocytes were positive in the 250-ng group (J). ABC method, Mayer's hematoxylin counterstain. Magnification ×140.

be determined why the 250-ng group showed higher CYP1B1 expression than the 7.5-μg group.

After DMBA was ingested to rats, previous studies have described the maximum urinary excretions of DMBA take place during the period ranging from 6 h to 1 day (Semin et al., 1976), and high levels of metabolite DMBA-DNA adducts in liver are found on days 1 to 2 (El-Bayoumy et al., 1992). Then, the large amounts of DMBA-DNA adducts in liver and mammary glands were remained to be observed at 12 days after DMBA ingestion (Daniel and Joyce, 1984), but their levels after that was unclear. Meanwhile, several previous studies have described the induction of rat hepatic CYP1 mRNA and/or protein within 1 day of DMBA ingestion (Badawi et al., 2000; Bolognesi et al., 1991; Granberg et al., 2000; Heidel et al., 1998; Moon et al., 1988; Rowlands et al., 2001). In our previous study, following DMBA ingestion without PCB126 exposure, the induction of hepatic CYP1A1 was first observed at 12 h, was revealed to peak on day 2 and decreased on day 5, and the induction of hepatic CYP1B1 was first observed on day 2 and decreased on day 5 (Muto et al., 2003). While present study revealed that prenatal PCB126 exposure rats were induced the prolongation of hepatic CYP1 induction following DMBA ingestion, especially the longer persistence of CYP1B1 induction was apparently in the 250-ng group. The implication of estradiol (E2) in breast tumorigenesis is widely documented (Nandi et al., 1995; Weinberg, 1996). An alternative mechanism of E2 carcinogenicity stems from the metabolism of this hormone, which generates several catechol derivatives from monohydroxylation reactions,